Applied Catalysis B: Environmental 306 (2022) 121059

Contents lists available at ScienceDirect

Applied Catalysis B: Environmental

journal homepage: www.elsevier.com/locate/apcatb

Selective hydrogenation catalyst made via heat-processing of biogenic Pd nanoparticles and novel 'green' catalyst for Heck coupling using waste sulfidogenic bacteria

Iryna P. Mikheenko [a], James A. Bennett [a,1], Jacob B. Omajali [a,2], Marc Walker [b], D. Barrie Johnson [c,d], Barry M. Grail [c], David Wong-Pascua [e], Jonathan D. Moseley [e,3], Lynne E. Macaskie [a,*]

[a] School of Biosciences, University of Birmingham, Birmingham B15 2TT, UK
[b] Department of Physics, University of Warwick, Coventry CV4 7AL, UK
[c] School of Natural Sciences, Bangor University, LL57 2UW, UK
[d] Faculty of Health and Life Sciences, Coventry University, Coventry CV1 5FB, UK
[e] CatSci Ltd, CBTC2, Capital Business Park, Wentloog, Cardiff CF3 2PX, UK

ARTICLE INFO

Keywords:
Palladium nanoparticle catalyst
Efficient hydrogenation
Heck synthesis
Waste upvalorization
Green chemistry

ABSTRACT

A heterogeneous Pd catalyst, biologically-mineralized palladium nanoparticles (bio-Pd), was synthesized using sulfidogenic bacteria which reduced soluble Pd(II) to catalytically-active Pd-nanoparticles (NPs). Heat treatment (processing) of bio-Pd (5 or 20 wt% on the cells) made by *Desulfovibrio desulfuricans* evolved supported Pd-catalyst comprising Pd-NPs held on large spherical hollow structures. The rate of hydrogenation of 2-butyne-1,4-diol was ~5-fold slower than for a commercial catalyst (~twice that of native bio-Pd), but with high selectivity to the alkene, fulfilling a key industrial criterion. In the Heck reaction, while bio-Pd showed a comparable reaction rate in ethyl cinnamate synthesis to that achieved by commercial Pd/C, heat-treated bio-Pd had negligible activity. *D. desulfuricans* bio-Pd was replaced by bio-Pd made using a consortium of waste acidophilic sulfidogenic bacteria (CAS) supplied from an unrelated primary remediation process. This gave comparable activity to commercial 5 wt% Pd/C in ethyl cinnamate synthesis, signposting an economic, scalable route to catalyst manufacture.

1. Introduction

Palladium nanoparticles supported on dead bacterial cells (bio-Pd) have shown excellent catalytic properties in a number of environmentally-relevant reactions which include fuel cell electrocatalysis, degradation of pollutants, oil upgrading and green chemistry [1–4]. This class of catalysts is unique; although a bio-derived support is used and catalyst synthesis uses living cells to initiate the metallic nanoparticles, the formation of metallic NPs kills the cells due to the harsh conditions and metal toxicity. For use membrane materials are removed to leave NPs supported on the residual organic matrix, which becomes analogous to other heterogeneous catalysts supported on various organic matrices. The 'choice' of the bacteria used in the NP synthetic reactions dictates the structure of the catalyst support matrix and patterning of the NPs, as well as organic and inorganic ligands which become associated with the finished catalytic nanoparticles.

Since the early 2000's various publications have suggested the possible commercial application of bio-Pd but traditional Pd catalysts are very well established over many years using well established manufacturing processes. For a new technology to gain acceptance it

* Corresponding author.
E-mail addresses: i.mikheenko@bham.ac.uk (I.P. Mikheenko), jamesbennett2@nottingham.ac.uk (J.A. Bennett), jomajali@tru.ca (J.B. Omajali), m.walker@warwick.ac.uk (M. Walker), d.b.johnson@bangor.ac.uk (D.B. Johnson), b.m.grail@btinternet.com (B.M. Grail), david.wong-pascua@catsci.com (D. Wong-Pascua), jonathan@scientificupdate.com (J.D. Moseley), l.e.macaskie@bham.ac.uk (L.E. Macaskie).
[1] Current address: School of Chemistry, University of Nottingham, Nottingham NG72RD, UK.
[2] Current address: Department of Chemistry, Thompson Rivers University, Kamloops, Canada.
[3] Current address: Scientific Update, Maycroft Place, Mayfield TN20 6EW, UK.

https://doi.org/10.1016/j.apcatb.2021.121059
Received 14 October 2021; Received in revised form 24 December 2021; Accepted 30 December 2021
Available online 4 January 2022

must be demonstrably better than existing counterparts or significantly cheaper without compromising performance (J. Clipsham and P. Claes; Catalytic Technology Management Ltd., unpublished report commissioned in 2009). This prompted the first Life Cycle Analysis (LCA) by Archer et al. [5] who concluded that platinum group metal (PGM) catalysts, biorefined from waste leachate into neo-catalyst, outperformed traditional heavy oil upgrading catalysts in terms of economic advantages, even without factoring-in the significant additional carbon and energy savings [3] via avoidance of metal extraction from primary ores. However, the composition of a bio-recovered metallic catalyst reflects the metallic composition of the original waste [6] and hence this approach, essentially making a potentially variable material, may be of limited use in chemical synthesis where a reproducibly high reaction selectivity is required, along with a high conversion efficiency.

In high value product syntheses, variable catalyst quality and the presence of extraneous elements is unacceptable and these must be removed from the final product stream post-reaction. Importantly, it is essential to remove toxic metals, especially PGMs, to negligible levels in pharmaceuticals to protect patients. Moreover, variable ratios of mixed metals, leading to variable product quality, would not be permitted for regulatory processes, nor would they provide reliable protocols and processes that could be claimed for successful patent filing. Even for the low value product industries, the metal/catalyst would need to be recovered for economic and environmental purposes. Pd-nanoparticles are tightly held (immobilized) on bacterial cells and were retained after repeated reaction cycles with no leaching of Pd, whereas this disadvantage occurred with commercial catalyst [7]. Taking this further, self-immobilization of the catalyst within highly self-adhesive biofilm has shown the potential for continuous flow-through processes [8,9], which rely upon catalyst stability.

As a sustainable approach towards the economy of catalyst synthesis, bio-Pd has been made using *Escherichia coli* sourced as waste from a primary biohydrogen process [10]. This biomaterial was catalytically active as a hydrogenation catalyst; when compared to a commercial 5% Pd on Al_2O_3 catalyst the reaction rate was lower but the selectivity to the desired product, 2-pentene, was higher [10].

The selective hydrogenation of 2-butyne-1,4-diol (Fig. 1) is an industrially-relevant model reaction as the partial-hydrogenation product, 2-butene-1,4-diol, is an intermediate in the production of several pharmaceuticals and pesticides [11]. However this reaction, over a variety of nickel and nickel–copper based catalysts under harsh conditions, leads to the production of butane-1,4-diol [12–14], whereas the use of milder conditions and deactivated precious metal catalysts, such as palladium on calcium carbonate, increases the selectivity towards *cis*-2-butene-1,4-diol. Winterbottom et al. [14] illustrated a general reaction scheme for the reaction. In addition to the partial and full hydrogenation products, 2-butene-1,4-diol and butanediol, a number of additional side-products may also be formed due to the isomerization of 2-butene-1,4-diol to γ-hydroxybutyraldehyde (Fig. 1). This isomerization was observed over Pd/C catalysts [13,15] with acidic conditions favoring isomerization and hydrogenolysis products [16]. Increased selectivities to 2-butene-1,4-diol were promoted by addition of base or basic support materials [17,18] though, in general, additions should be avoided for economic reasons and waste minimization.

Another important reaction which employs palladium catalysts is the Heck reaction, in which an alkene is coupled with an aryl- or alkenyl-halide to produce vinylarenes or dienes [19,20]. Traditionally this reaction has employed homogeneous catalysis [19,21] but using ligand-free Pd heterogeneous catalysts can be more advantageous [22] and hence these are extensively researched [23], with use of microbial cells as a more recent addition to the portfolio of supports that combine the benefits of homo-and heterogeneous catalysts [24]. A commonly used supported catalyst, Pd/SiO_2 is considered uncompetitive against homogeneous Pd catalysts due to its low activity as compared to the latter [25]. Huang et al. [22] reported a Pd/SiO_2 catalyst that was highly active for the Heck coupling, attributed to the size effect of supported Pd particles, generated in situ from Pd^{2+}/SiO_2. More recent developments used 'bio-Pd' made in situ from Pd(II) by various types of bacteria which was shown to be active in the Heck coupling when tested under industrially-relevant conditions against an established comparator [4].

Early work showed that, for a bio-Pd fuel cell (FC) electrocatalyst, it was necessary to carbonize the cells by heat treatment in order to obtain conductivity [26] since biomass (a hydrated polymeric biomatrix) is mostly water. Electron paramagnetic resonance (EPR) studies of bio-Pd NPs evolved on carbonized, heat-treated biomass showed single electron transfer reactions with bio-Pd made on *Escherichia coli* and *Desulfovibrio desulfuricans*, with a higher electron transfer via the latter [27] corresponding to higher catalytic activity as a FC catalyst [26,28]. This prompted evaluation of heat-processing of bio-Pd to potentially increase its performance more generally, which formed the first objective of this study using two test reactions: the selective hydrogenation of 2-butyne-1,4-diol and the Heck reaction of ethyl cinnamate from ethyl

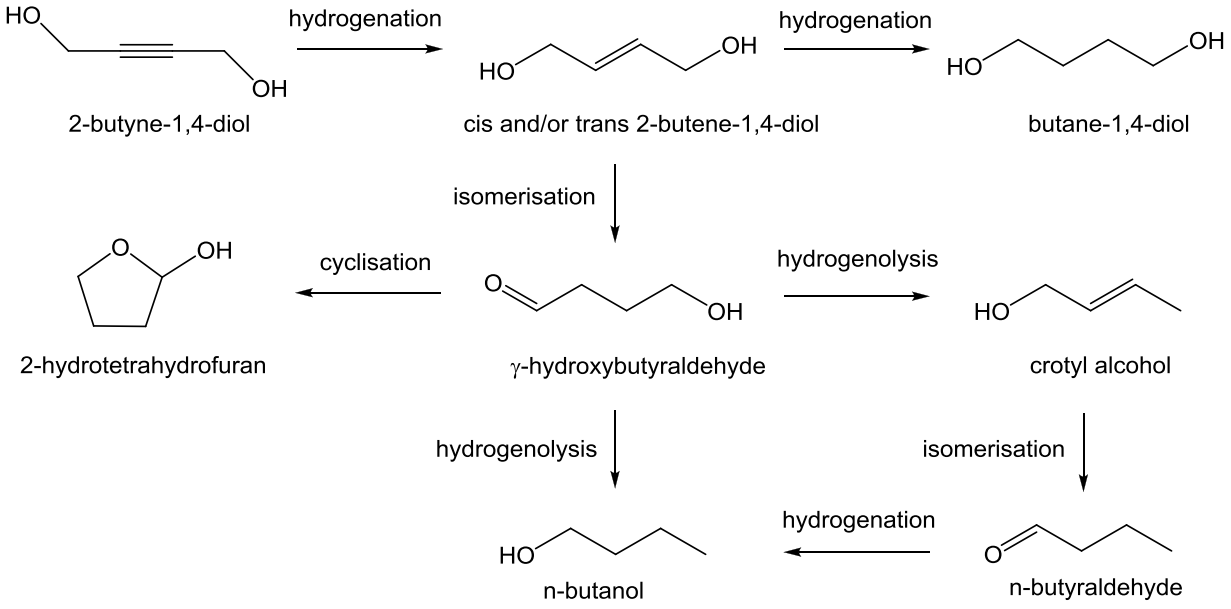

Fig. 1. Reaction scheme for the hydrogenation of 2-butyne-1,4-diol.

acrylate using palladized cells of *D. desulfuricans*. This was chosen as the model organism since, in addition to the EPR study (above), early work showed that the bio-Pd made on *Desulfovibrio* cells is highly active catalytically [4], attributed to the high activity of hydrogenases which are implicated in the reduction of Pd(II) to form well-patterned, bio--scaffolded Pd(0) nanoparticles (NPs) [29,30].

Desulfovibrio spp. are sulfidogens, and respire on sulfate in the absence of oxygen to produce H_2S. A mixed consortium of acidophilic sulfidogenic (CAS) bacteria has been used to recover metals (e.g. Zn, Cu) from synthetic acid mine drainage (AMD) waters via evolved biogenic H_2S from the culture as a metal precipitant off-line (cited in [31]). The residual CAS cells (which have not been exposed to heavy metals) comprise an uncontaminated biomass waste, potentially produced at large scale, which requires disposal at cost with potential for adverse environmental impact. This prompted consideration of CAS bacteria as the support for bio-Pd. Hence, the second objective of this study was to compare the catalytic activity of bio-Pd supported on *D. desulfuricans* with comparable Pd-NPs supported on waste CAS cells in the Heck reaction as a paradigm for 'green catalyst from waste'. A biohydrogen process previously shown to yield waste bacteria is at proof of concept stage with respect to use of the biowaste in 'second life' as a bio-Pd hydrogenation catalyst [10] but biohydrogen technologies are still not well developed. In contrast, while not yet upscaled, the mine water remediation process has been demonstrated against real wastewaters. The volume of acid mine drainage, continuously produced as mine water runoff, is large (e.g. $>$ 10 million litres/day) and hence CAS would be continuously generated in large quantities [3] with biomass waste management and mitigation becoming significant factors in overall process economics.

In order to address the two independent criteria for bio-Pd to become commercially competitive, as articulated from the viewpoint of the precious metals and catalysis industries (Clipsham and Claes, unpublished, above; which did not factor-in environmental benefits), the dual illustrative goals of this study were to increase the activity of the paradigm bio-Pd catalyst of *D. desulfuricans* by heat processing and to offset the catalyst cost by the illustrative use of CAS waste bacteria for manufacturing of catalytic NPs.

Traditionally, for process evaluation, a Life Cycle Analysis (LCA) is made within defined system boundaries that factor-in only techno-economic factors, as illustrated by the use of bio-Pd biorefined from metallic wastes to upgrade heavy oil (see [5]). In this example the set boundaries excluded the environmental mitigation offered by cleaner oil production at source as well as the reduced temperature (energy demand) required for downstream refinery of the lower viscosity oil. In the context of bio-Pd catalyst applied to the chemical industry competitiveness of new technology is currently considered only on the basis of the two criteria outlined above. However, in the wider context two additional key factors must be taken into account within the system boundaries, namely: (i) a reaction that produces better selectivity requires less starting material for a given yield of desired product; in the case of 2-pentyne hydrogenation (for example) that equates to a saving in petrochemically-derived 2-pentyne feedstock, while (ii): a smaller amount of unwanted by-product gives less waste for treatment/disposal. A further factor is that Pd-nanoparticles supported on bacterial cells can be easily recovered from the reaction (above) while the use of biofilm-catalyst conveniently allows flow-through continuous processes that can be imaged directly in 4-D and mathematically modelled [8] to facilitate process optimization and highlight bottlenecks. These factors (cleaner production, greater materials/process efficiency, less waste) should also be calculated-in, with reference also to a numerical value assigned to carbon mitigation, factors which are being only now incorporated to augment LCA analyses to evaluate traditional and new technologies on a 'level playing field' to quantify the drivers for change towards circularity and climate change mitigation. Without such drivers changes in industrial practices (against 'business as usual') will not be adopted.

2. Experimental

2.1. Bacterial strains, cultivation conditions and bio-Pd preparation

For the hydrogenation tests and trials in the Heck reaction *D. desulfuricans* NCIMB 8307 was grown anaerobically in Postgate C medium at 30 °C [4] and harvested by centrifugation. After washing in MOPS-NaOH buffer pH 7.0 three times and storing at 4 °C under oxygen-free nitrogen (OFN) the biomass was palladized as described by Deplanche et al. [4] using Na_2PdCl_4 solution in 0.01 M HNO_3 with the Pd(II) initially biosorbed onto the bacterial cells then reduced to Pd(0) enzymatically under H_2 [4]. By pre-setting the proportions of resting live cells (calculated as dry biomass, obtained by a previously-determined conversion) to Pd(II) two mass loadings (5 wt% and 20 wt% Pd/cell dry wt) of Pd onto biomass were used (adjusting the proportions of Pd (II):biomass as required; all of the Pd(II) was removed from the solution by assay). Part of the sample was retained for examination using electron microscopy, X-ray photoelectron spectroscopy (XPS) and X-ray powder diffraction (XRD). Palladized cells (bio-Pd) were air-dried and ground in an agate mortar. One part of the preparation was used as a catalyst directly and another part was subjected to heat treatment before testing.

The consortium of acidophilic sulfidogenic (CAS) bacteria was taken from a continuous metal waste treatment process where the H_2S off-gas was removed from a continuous flow bioreactor and gassed into acidic, metal-rich mine water in order to selectively precipitate target transition metals [31] to leave residual (uncontaminated) biomass in the parent vessel. The CAS samples were harvested by centrifugation from this continuous culture, washed as for *D. desulfuricans* and stored as a concentrated suspension at 4 °C under air, routinely overnight before palladization. The CAS comprised 66% *Desulfosporosinus acididurans* [32], 7% Firmicute strain CEB3, 10% *Acidocella aromatica* strain PFBC, 10% *Actinobacterium* AR3 and 7% *Acidithiobacillus ferrooxidans* [33]. An electron microscope study of the CAS culture post-metallization [31] previously showed no extracellular precipitation of metals onto (e.g) cell-associated slimes. The cells were processed and tested alongside the sulfidogenic comparator, *D. desulfuricans*, NCIMB 8307 (both cultures to 5 wt% Pd [31]).

2.2. Preparation of heat-treated catalyst on D. desulfuricans

Heat treated catalyst was prepared in this study using the paradigm *D. desulfuricans* catalyst (CAS bacteria were not heat treated). The sample (20 wt% or 5 wt% Pd; 200 – 500 mg) was placed into a ceramic boat, wrapped in a steel foil and placed into a furnace (Eurotherm, Lenton Thermal Designs Ltd). After reaching vacuum (8×10^{-5} mbar) the temperature was increased (10 °C/min) to 960 °C and maintained for 1 h. The pressure was monitored during heating. Samples were left to cool slowly. The samples obtained (dark-grey powder) were used for catalytic testing in intact and ground forms; both gave similar results.

2.3. Pd assay in depleted medium and bio-Pd carbonized preparations

Complete removal of Pd from the suspension was confirmed by assay (below) to confirm complete Pd loading on the cells. To estimate the quantity of Pd held on the carbonized material formed by sintering (in order to compare reactions on a mol Pd basis) sample (10 mg) was mixed with *aqua regia* (5 mL) and heated to 100 °C. The mixture was evaporated and wet crystals re-dissolved in 5 mL distilled water. After centrifugation, the Pd(II) concentration was estimated spectrophotometrically with $SnCl_2$ [34].

2.4. Examination of palladized bacteria and heated biomaterial by electron microscopy, energy dispersive X-ray analysis (EDX) and X-ray powder diffraction (XRD)

Pd-loaded bacteria were fixed and stained with 1% osmium tetraoxide following standard procedures with sections viewed with a JEOL 120CX2 transmission electron microscope and analyzed by EDX [29,35–37]. Samples of Pd-loaded bacteria and carbonized bio-Pd were also examined using a Philips XL-30 FEG environmental scanning electron microscope, accelerating voltage 10 kV. Selected samples were examined by EDX. X-ray diffraction powder patterns (bulk method) were acquired via a Siemens High Resolution Powder Diffractometer (wavelength 0.154 nm), compared with the lines of pure palladium and checked against a previous report [36] and reference database.

2.5. Analysis of Pd-loaded bacteria by X-ray photoelectron spectroscopy (XPS)

XPS provides key information about the chemistry of the outermost 5–10 nm of a sample via binding energies between atoms [38], quantified as chemical shifts in binding energies, to identify an atom and its oxidation state or chemical interaction with neighbouring atoms. Prior to XPS examination, sample aliquots (5–10 mg of material) were dried on a boron-doped silicon wafer (7 ×7 mm in diameter). X-ray photoelectron spectroscopy (XPS) data were collected at the Science City Photoemission Facility, University of Warwick, UK. Samples were mounted on Omicron sample plates (via electrically conductive carbon tape) and placed in a fast-entry chamber. The pressure was reduced to less than 1×10^{-7} mbar (approx. 1 h), and the samples were transferred under vacuum to a storage carousel, located between the preparation and main analysis chambers, for storage at pressures of less than 2×10^{-10} mbar. XPS data were collected in the main analysis chamber (base pressure 2×10^{-11} mbar), under illumination via an XM1000 monochromatic Al $K\alpha_\alpha$ X-ray source (Omicron Nanotechnology). Measurements were made at room temperature and take-off angle of 90° (maximum probe depth of ~ 5–10 nm). Emitted photoelectrons were detected using a Sphera electron analyser (Omicron Nanotechnology), with the core levels recorded using a pass energy of 10 eV (resolution ~ 0.47 eV). Due to the insulating nature of hydrated biomaterial, a CN10 charge neutralizer (Omicron Nanotechnology) was used to prevent surface charging, whereby a low energy (typically 1.5 eV) beam of electrons was directed on to the sample during XPS data acquisition. Data were converted into VAMAS format and analyzed using the CasaXPS package, using Shirley backgrounds, mixed Gaussian-Lorentzian (Voigt) line-shapes and asymmetry parameters where appropriate. Binding energies were calibrated to the C 1 s peaks originating from adventitious carbon at 284.6 eV. Samples examined were palladium solution (background) and cells exposed to Pd(II) ions (i.e. biosorbed metal) and following in situ reduction of sorbed Pd(II) to Pd-NPs. Reduction of sorbed Pd(II) inside the XPS instrument was achieved in the sample preparation chamber by flowing H_2 gas over the filament of a TC-50 thermal gas cracker (Oxford Applied Research), running at 58 W, in order to produce atomic hydrogen which was subsequently directed onto the sample surface. The sample was then transferred back to the analysis chamber, under ultra-high vacuum, for the subsequent acquisition of XP spectra.

2.6. Test reactions

2.6.1. Hydrogenation

The reactions were run in a 500 mL high pressure stainless steel autoclave reactor (Baskerville Ltd.; pressure of 2 bar and temperature of 40 °C). 300 mL of 0.72% 2-butyne-1,4-diol (Sigma-Aldrich Ltd.) solution in 2-propanol (Fisher Scientific UK) was put into the vessel with catalyst (0.205 mol% Pd over the substrate). As the heated bio-Pd sample had lost mass (estimated thermogravimetrically: [39]) the relative Pd content/g (wt% Pd) increased and hence a constant mol% Pd was used to encompass this. For the reaction the reactor was purged with nitrogen and the reaction was initiated by addition of H_2. Samples of the reaction mixture (stirred at 1000 rpm) were taken at 10 min intervals during the first half hour, then at 30 min intervals thereafter. The comparator was commercial 5% Pd/alumina. Sample analysis was performed by gas chromatography, using a Varian CP-3380 with a flame ionization detector and a 25 M Chrompack Plot CP7576 capillary column with an Al_2O_3/KCl coating. The oven temperature ramp used was as follows: initial temperature of 95 °C for 30 min, ramp to 220 °C at 50 °C/min, hold 20 min. An injection volume of 0.1 μL was used.

2.6.2. Heck reaction (Heck coupling reaction between iodobenzene and ethyl acrylate)

Method 1 was used to compare native and heat-processed samples of bio-Pd on *D. desulfuricans* with the comparator being commercial 5 wt% Pd/C. Iodobenzene (408 mg in 30 mL of dimethylformamide), 0.4 mL triethylamine and catalyst (0.205 mol% Pd/substrate) were placed into a 2-neck round bottomed flask (50 mL) under OFN. The mixture was placed in a pre-heated oil bath (120 °C) and stirred vigorously. The reaction was initiated by addition of 0.3 mL of ethyl acrylate. Timed samples were withdrawn over 4 h. Reaction products were analyzed by HPLC (Phenomenex, Utrecht, NL) in a water-acetonitrile gradient and absorbance detector (230 nm). Method 2 was used to compare bio-Pd on *D. desulfuricans* and CAS bacteria, the comparator being 5 wt% Pd/C. Catalysts (10.6 mg, 5 wt% Pd, 0.5 mol% loading) were dispensed into Radleys carousel tubes under N_2 in a glovebox. A stock solution of iodobenzene (66.7 mM, 13.6 mg/mL) and ethyl acrylate (100.0 mM, 10.0 mg/mL) in dimethylformamide was prepared and aliquots (15 mL) transferred to the Radleys tubes containing catalyst. The tubes were sealed and placed into a carousel with a heating block and condensing head outside the glovebox. Reactions were stirred and heated to 80 °C and the reaction was initiated by the addition of triethylamine (152 mg). Reactions were sampled at time intervals and analyzed. The Radleys tubes were vented with nitrogen during addition of base and sampling. Analysis was by UV-UPLC (Waters: i-class UPLC with TQD; BEH column RP18 in a gradient of 0.03% trifluoroacetic acid 100% water and 0.03% trifluoroacetic acid 100% acetonitrile) 4 min run time flow rate 0.7 mL/min with diode array detection (210–400 nm).

3. Results

3.1. Examination of D. desulfuricans cells and supported palladium nanoparticles

The formation of Pd-NPs on cells of paradigm *D. desulfuricans* was reported previously (e.g. see [29,31,35,37,40]. Examination of the Pd-loaded cells in this study by environmental scanning electron microscopy (via electron back scattering) shows the Pd-NPs (white dots) standing proud of the cells (Fig. 2a). Without added palladium cell sections examined by transmission electron microscopy show no nanoparticles (Fig. 2b, inset) but following palladization Pd-NPs are visible in cell sections on the cell surface and also embedded in the cell surface layers (Fig. 2b). Further examination of cells loaded at 20 wt% Pd (Fig. 2c) shows extrusion of electron opaque NP clusters (identified as Pd by EDX :not shown) through the outer membrane and extending beyond the cell. The extrusions, (which have visible cell surface debris attached) appear to relate to location of Pd-foci in the inner membrane and also traverse the periplasmic space which suggests a possible functional relationship between the mediating hydrogenases (inner membrane and periplasmically-located) and their ability to promote Pd(II) reduction [29] but this was not examined further. It is likely that at 20 wt% loading the NPs had agglomerated but the ‘bunches of grapes’ appearance and detectable membrane fragments (Fig. 2c) suggests some stabilization of component small NPs but this was not examined further. The CAS bacteria were not examined here due to the difficulty of

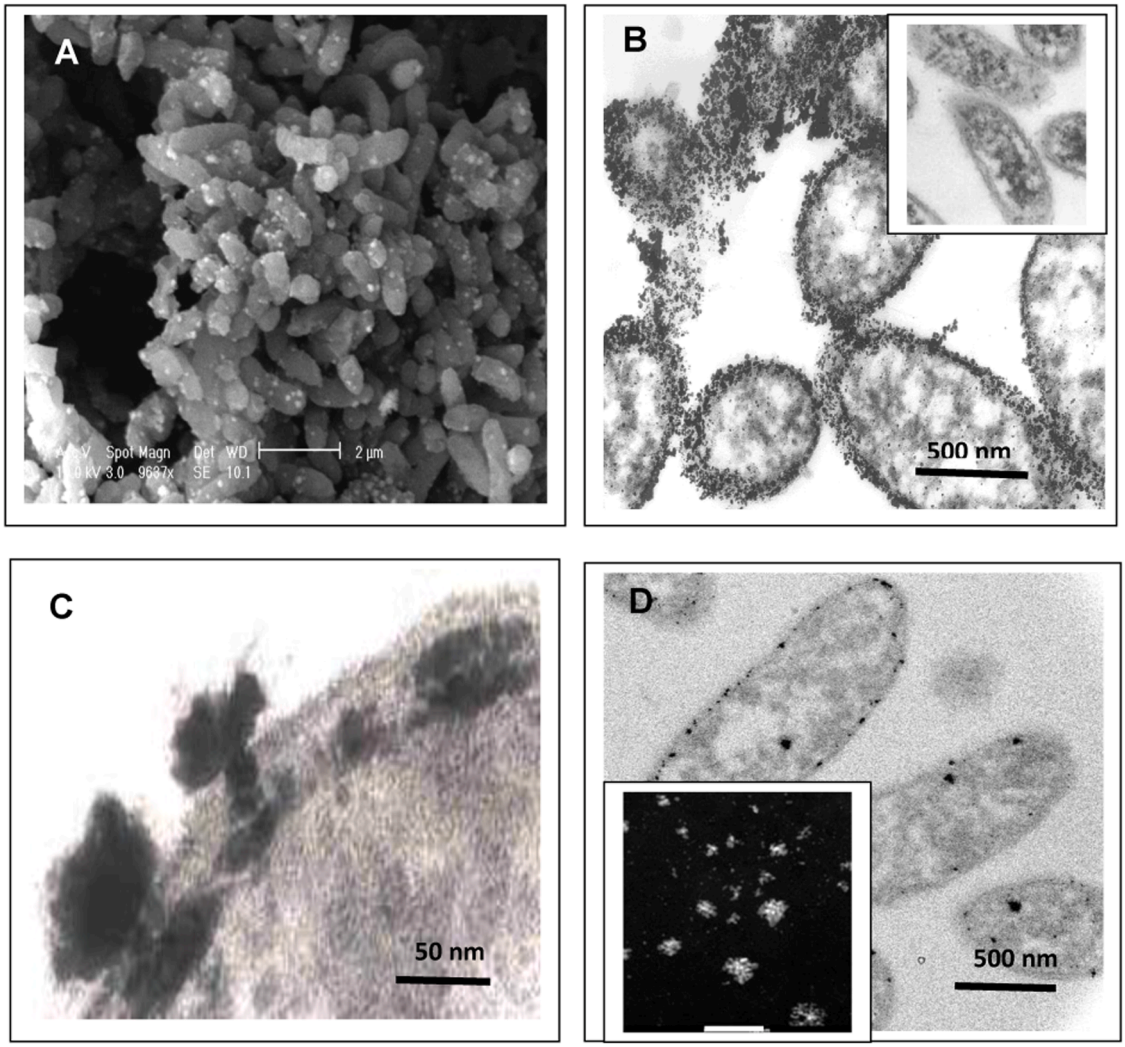

Fig. 2. Palladized cells of *D. desulfuricans* viewed by ESEM (A) and TEM (B,C) at 20 wt (B,C) and at 5 wt% (D) with a dark field image (inset; bar is 50 nm) showing that larger NPs are agglomerations of smaller ones. B, inset: unchallenged cells.

interpretation due to the culture heterogeneity; example electron micrographs (showing 3 main types of cells) were published previously [31], showing that, in contrast to *D. desulfuricans*, Pd NPs were localized intracellularly.

Examination of cells loaded to 5 wt% Pd confirms that the Pd-NPs were held mainly within the cell surface layers (Fig. 2d). Examination of intracellular material shows negligible Pd-NPs (Fig. 2d) but the relatively low resolution as used for the images of Fig. 2 could not preclude the occurrence of very small intracellular NPs, subsequently revealed in a related study via high resolution electron microscopy [40]. The latter confirmed the predominance of Pd-NPs at the cell surface in *D. desulfuricans* (i.e. accessible for catalysis in native cells) whereas in the case of *E. coli* they were located at the cell surface, and also intracellularly [40]. In accordance with previous work [37] Fig. 2d suggests association of intracellular electron opaque material with nuclear bodies, which suggests some uptake of Pd(II) into the cells despite the apparent paucity of intracellular NPs. Examination of the surface of a cell populated by Pd-NPs shows that, while some NPs were small and separated, larger NPs were evident, being agglomerations of smaller ones (Fig. 2d, inset).

Examination of the bio-Pd by X-ray powder diffraction gave a powder pattern corresponding to the diffraction lines of palladium as described previously [39] (example shown in Supplementary Information Fig. S1). A poor peak resolution of native bio-Pd suggested Pd which was mostly amorphous. Application of the Scherrer equation (to analyze the crystalline components) gave crystallite sizes of 3.3 and 4.6 nm for 5 wt% Pd and 13.1 and 8.6 nm for 20 wt% Pd (from two independent cultures of *D. desulfuricans* examined several years apart). This would seem to contradict the appearance of the large clusters as shown in Fig. 2c but close examination indicates the Pd-clusters to be agglomerations of small Pd-NPs (Fig. 2c, d, inset), possibly stabilized by residual associated outer membrane materials, visible as indistinct cellular extrusions in association with the NPs in Fig. 2c. Association between Pd-NPs and biomatrix components was confirmed previously [41].

A companion study [40] applied high resolution electron microscopy with elemental mapping to reveal co-localization of Pd and sulfur in palladized cells of *D. desulfuricans* (5 wt% Pd). Numerical analysis gave a Mander's overlap coefficient of > 0.9 for Pd and S and also Pd and P, confirming co-localization of Pd with cellular components containing these elements. This is in accordance with previous work that showed co-localized Pd and S in a nuclear body of *D. desulfuricans* [36,37] which implied binding of Pd(II) to histone-like proteins associated with DNA (via protein sulfhydryl groups), while the phosphate groups of DNA would be likely targets for binding of Pd(II), along with membrane phospholipids encountered as the Pd(II) enters the cells. Thus, while Pd was localized at the cell surface (and found also in nuclear bodies), unlike in the case of *E. coli* [40] the cytoplasm of *D. desulfuricans* was Pd-sparse (Fig. 2d), which has positive implications for better

accessibility of the Pd(0) (surface-localized) to incoming substrates for catalysis. This sparsity cannot necessarily be taken to indicate a lack of uptake of Pd(II) by the cells; Gram negative bacteria have well established metal efflux mechanisms to moderate metal toxicity while controlling the availability of essential trace metals. A rapid method to visualize altered Pd accumulation by *E. coli* [42] showed influential effects of several genes related to transport/efflux of copper, silver, cobalt, molybdenum and iron(II) but a similar study has not been done in the case of *D. desulfuricans*.

3.2. Analysis of Pd at the cell surface of *D. desulfuricans* by X ray photoelectron spectroscopy

The bacterial outer membrane contains, in addition to membrane phospholipids, a significant protein content (approx. 50% of the outer membrane material: see [43]). XPS spectra of the cell surface of *D. desulfuricans* (before Pd addition) are shown in Supplementary Information Fig. S2. Potential coordination sites for incoming Pd(II) include (as shown by XPS) oxygen and nitrogen ligands [44] via a preliminary study using cells examined at the initial stages of Pd(II) sorption. Binding of Pd(II) to phosphorus and sulfur was not examined in that earlier work. XPS spectra are shown in Fig. 3b for *D. desulfuricans*-Pd cells with peak assignments for carbon (Fig. 3c), nitrogen (Fig. 3d),

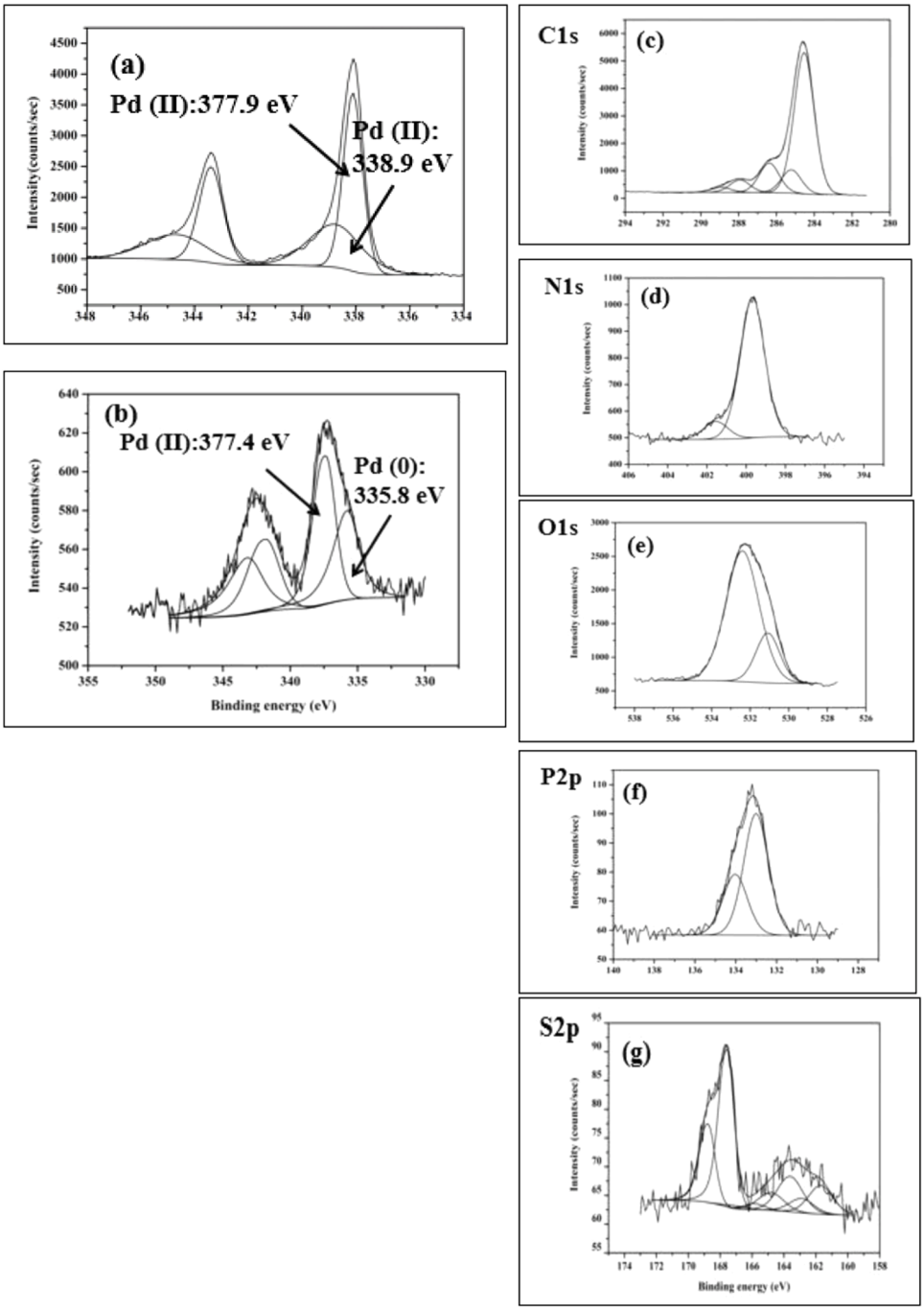

Fig. 3. XPS spectra of Pd solution (a) and cells of *D. desulfuricans* (b) following in situ reduction of Pd(II). Note that Pd3d peaks appear as doublets. XPS spectra are shown post reduction for: C (c), N (d), O (e) P (f) and S (g). Reference spectra for the native (unpalladized) cells are shown in Supplementary Information Fig. S2.

oxygen (Fig. 3e), phosphorus (Fig. 3f) and sulfur (Fig. 3g). Whereas the previous study [44] reported that in the presence of atmospheric oxygen the main species in Pd(II) chloride solution were PdO, Pd-OH, Pd-Cl and species with a possible intermediate state between Pd(0) and Pd(II), Omajali [36] reported only Pd(II) in a nitrate-solution matrix as used in this work. The spectrum of the Pd(II) solution is shown in Fig. 3a together with the corresponding Pd species in the reduced bio-Pd. This material was reduced abiotically with hydrogen in situ, resulting in the typical doublet (335.8 eV and 341.1 eV) of Pd(0) (Fig. 3b). This result was similar to that obtained using cells that were allowed to reduce Pd (II) under hydrogen and then introduced into the spectrometer post-reduction [36]. However reduction in situ discounts possible changes in speciation of Pd occurring during sample storage and transfer.

By using the XPS data to calculate the total intensity observed in each region and adjusting for their relative sensitivities, the atom % of the outermost cell surface layer was estimated (Table 1) to comprise nearly 80% carbon, with oxygen attributable to the cell surface materials that contain carboxyl groups (e.g. cell surface lipopolysaccharides and also (lipo) proteins), in addition to adsorbed atmospheric contaminants. The phosphorus can be attributed to the phospholipid outer membrane. The nitrogen (4.3 atom %) is attributed to proteins in the outer wall layers/outer membrane and the sulfur (~ 0.3 atom %) to sulfhydryl and thiol groups. This low abundance is in accordance with the occurrence of the S-containing amino acids cysteine and methionine (i.e. together nominally comprising ~ 10% of the total of 20 amino acids); an amino acid analysis of the cell surface proteins was not performed (these are very well known, e.g. [43]) but the abundance of sulfur-ligands suggests potential coordination sites for incoming Pd(II). It is important to note that this atomic concentration reflects the outermost few nm of the cell surface and does not inform about the sulfur content of materials beneath the outermost surface, i.e. in inner membrane-bound and periplasmically-facing NPs as evident in Fig. 2c.

Omajali [36] showed that the binding energy of $S2p_{3/2}$ on the cell of *D. desulfuricans* prior to metallization was 165.4 eV with a corresponding $S2p_{1/2}$ peak of 167.4 eV. In this current study, when Pd(II) was added onto bacterial cells and reduced in situ, there was a shift to lower binding energies; the pair 161.9 eV and 163.3 eV (Fig. 3g) suggest the formation of a Pd-S bond [45], in addition to other pairs which may be due to thiols, sulfates and organic sulfur (Fig. 3g) found on the bacterial cell. Since *D. desulfuricans* is a sulfidogen (and, indeed, metal sulfide production may comprise a resistance mechanism), the possibility of residual H_2S generated during pre-growth cannot be precluded. However, the bacteria had been washed three times before Pd-exposure and they were not provided with SO_4^{2-} into the resting cell suspension prior to this. Nevertheless, protein degradation and turnover in resting cells can be a source of low levels of H_2S; this was not evaluated in the present study.

3.3. Effect of heat treatment on bio-Pd material

Heat treatment of the bio-Pd resulted in loss of cell structures, and hollow spheres were apparent of size ~50–500 μm (Fig. 4a,b). Heat treatment of carbonaceous materials is a well-recognized route to the synthesis of hollow carbon spheres [46] while thermogravimetric analysis of bio-Pd showed loss of the bound water and labile biochemical components (polysaccharides, proteins) to leave the residual mineral and carbon components [39]. Close examination of a single sphere (Fig. 4c) shows the surface to be populated with small particles (~ 2–4 μm) with a small number of small NPs often associated with the surface of the larger particles (Fig. 4d); upon the latter clear facets are apparent. The carbon spheres derived from 20 wt% bio-Pd supported two subsets of clusters: 20–100 nm and 500 – 2000 nm, while the larger Pd cluster size on the spheres derived from 5 wt% bio-Pd was smaller than the latter, in the range of 100–600 nm (not shown). Close examination showed that three nanoparticle species were present, the large NPs, smaller ones associated with them and very small 'orphan' NPs (circled in Fig. 4e). The high temperature used would result in loss of organic materials and also H_2S, although heat treatment has also been recently-reported to convert sulfur-rich PdS into a sulfur-lean phase (Pd_4S) as volatile sulfur components are lost [47] which has implications for catalysis (see Discussion). EDX analysis of the material confirmed the presence of Pd but the presence of residual sulfur could not be confirmed unequivocally due to the close X-ray emission energies of Pd and S (Fig. 4f).

It is important to note that, while the bio-Pd was synthesized under H_2 and the heat processing was performed under vacuum, the samples were routinely stored in air prior to use as catalysts; the degree of Pd oxidation in storage was not determined. It is likely that the bio-Pd (regardless of the actual structure) functions as a catalyst to autodegrade cellular materials as the temperature is increased, e.g. membrane hydrocarbons may be converted into carbon nanostructures and/or evolve H_2 during catalytic 'cracking' that could result in the formation of palladium hydrides and carbides (see later Discussion).

3.4. Catalytic activity of native and heat-processed D. desulfuricans catalysts in hydrogenation of 2-butyne-1,4-diol

The hydrogenation of 2-butyne-1,4-diol catalyzed by a commercial 5 wt% Pd/alumina catalyst showed a rapid reaction (> 80% complete within 1 h) yielding only the fully hydrogenated 2-butane-1,4-diol following a transient appearance of 2-butene-1,4-diol during the first 30 min (Fig. 5a). Hence, the reaction was rapid but was unselective for the partially hydrogenated product using this catalyst.

Use of the 20 wt% Pd on *D. desulfuricans* gave a slower conversion rate (Fig. 5b), the commercial catalyst and the bio-Pd requiring ~25 min and 175 min, respectively for 50% conversion (Fig. 5a,b), which may have been attributable to NP agglomeration at the higher bio-Pd loading (see earlier). However, In contrast to the commercial catalyst, the native bio-Pd produced the alkene product in preference (~40% selectivity at 200 min), but also with significant amounts of the fully hydrogenated alkane (Fig. 5b).

The heat-treated (carbonized) derivative of the 20 wt% bio-Pd was tested (Fig. 5d). For catalytic testing the carbonized samples were used in two forms – as intact spheres (as in Fig. 4a–c) and as ground spheres; the two preparations gave similar results. Use of the heat-processed catalyst (with comparable mol loadings of Pd per reaction) gave an overall rate faster than with the native bio-Pd (50% conversion in ~125 min), while the main product was 2-butene-1,4-diol with a negligible amount of the fully hydrogenated alkane (Fig. 5d) (~80% selectivity after 200 min). Since use of 20 wt% Pd would be uneconomic commercially the catalyst was also tested using heat-treated 5 wt% bio-Pd (Fig. 5c). The conversion was slower than for the 20 wt% preparation (50% conversion in 180 min) but retained good selectivity to 2-butene-1,4-diol (~50% selectivity after 200 min) (Fig. 5c). However, comparing selectivities in incomplete reactions may not be reliable since they are not directly comparable; reduction to the butane can only happen after the butene has been formed, so will be slow initially when the butene concentration is low. If it is still low at the end then the selectivity is confirmed as good, i.e. as found with the heat treated

Table 1
Elemental composition of cell surface estimated by XPS spectra*.

Element	Atomic concentration (%)
C1s	77.6
N1s	4.3
O1s	17.4
P2p	0.65
S2p	0.26

* Spectra are shown in Supplementary Information Fig. S2

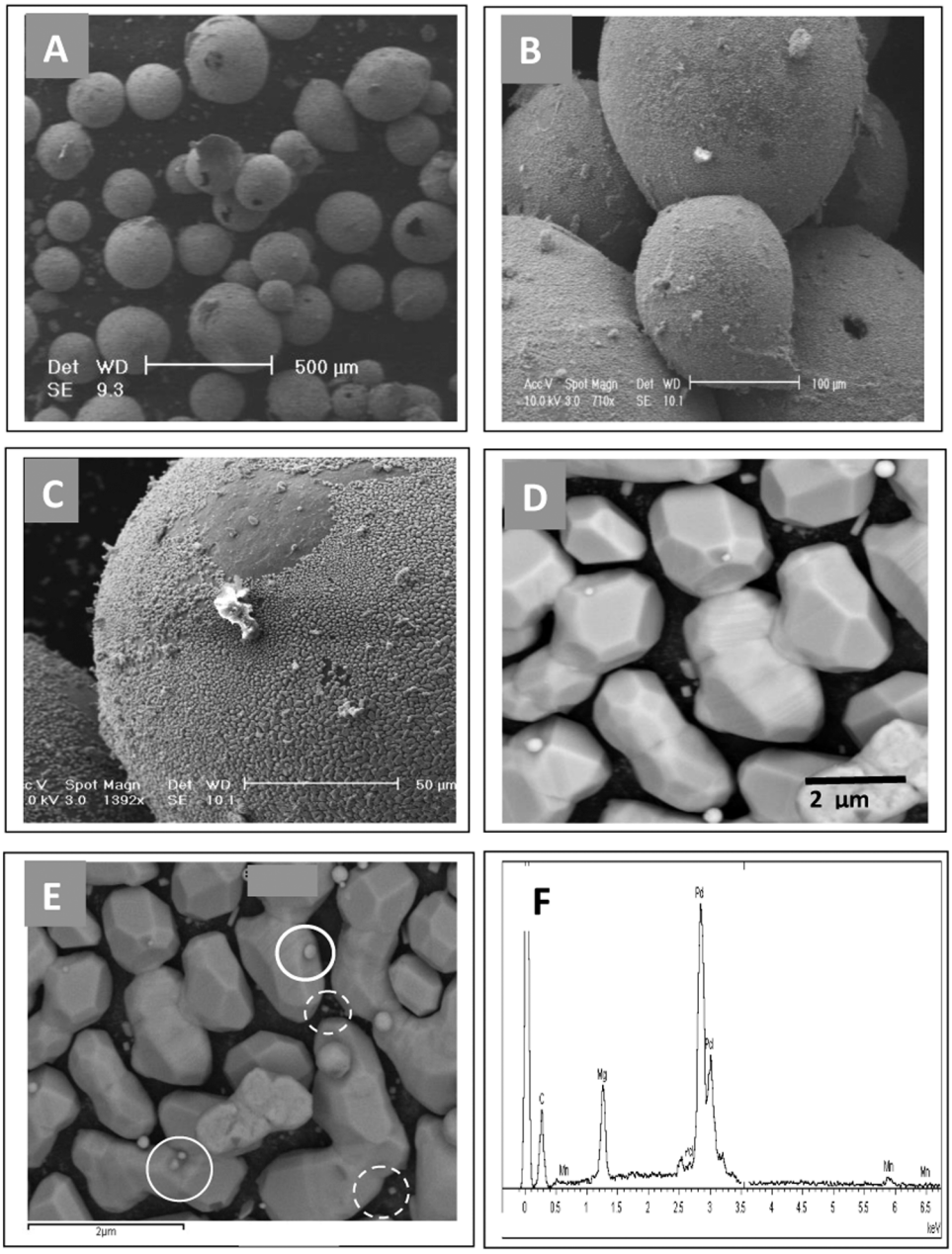

Fig. 4. Heat processed material produced from 20 wt% bio-Pd on *D. desulfuricans*. Hollow spheres are shown in A,B. The material is fragile, as evidenced by broken spheres in A. Intact and broken spheres gave similar results in catalytic tests. Note sample heterogeneity. Large Pd-particles predominate (D,E) and some appear to have outgrowths of small Pd-NPs (circled). In addition very small 'orphan' NPs are visible between the large NPs (broken circles) to give three NP populations. F: EDX analysis of the heat-treated material. As the X-ray emission of Pd Lα is 2.838 keV and the X-ray emission of S Kα is 2.307 keV these are not easily distinguished in EDX spectra.

material at 20 wt% and 5 wt% Pd loading (Fig. 5c,d). Hence it was concluded that, while use of bio-Pd confers product selectivity as compared to the commercial counterpart, heat processing of the bio-Pd catalyst achieved a higher selectivity not achieved with the commercial catalyst or with unprocessed bio-Pd. It should be noted that comparison of conversions and rates (mol/mg intact catalyst/min) are not meaningful when comparing the native and heat-processed biomaterial against the commercial catalyst as a significant proportion (~80%) of the mass of the biomaterial is lost in the heat treatment as shown by thermogravimetric analysis [39]. Hence, comparable amounts of Pd were introduced into each reaction to achieve realistic comparisons. It is not known the extent to which residual biomass carbon may remain functionally associated with the larger Pd particles (see Fig. 2), e.g. producing electronic interactions. Electron transfer between heat-treated bio-Pd NPs and activated carbon was reported previously using electron paramagnetic resonance [27].

We conclude that heat-processing of bio-Pd yielded a more selective catalyst for the hydrogenation of 2-butyne-1,4-diol than either native bio-Pd or a traditional supported Pd catalyst. This improvement could be attributed to a combination of Pd particle morphology and carbon-content, with large particles possessing a high proportion of the more thermally-stable and selective (111) terraces and a higher degree of subsurface C, leading to reduced subsurface H and minimized total-hydrogenation to the alkane (see Discussion).

3.5. *Catalytic activity of native and heat-processed D. desulfuricans catalysts in the Heck synthesis*

The Heck conversion of ethyl acrylate to ethyl cinnamate catalyzed by the various materials is shown in Fig. 6. Bio-Pd at 5 wt% Pd gave a similar conversion to 5 wt% Pd/C but this was approximately halved in the case of bio-Pd at 20 wt% Pd, i.e. the higher Pd loading on the cells worsens the reaction outcome, in contrast to the hydrogenation reaction (above). Notably, in marked contrast to the hydrogenation tests, the heat-processed bio-Pd catalysts had no activity (Fig. 6). It was concluded that for the Heck reaction (formation of C-C bonds) heat processing of

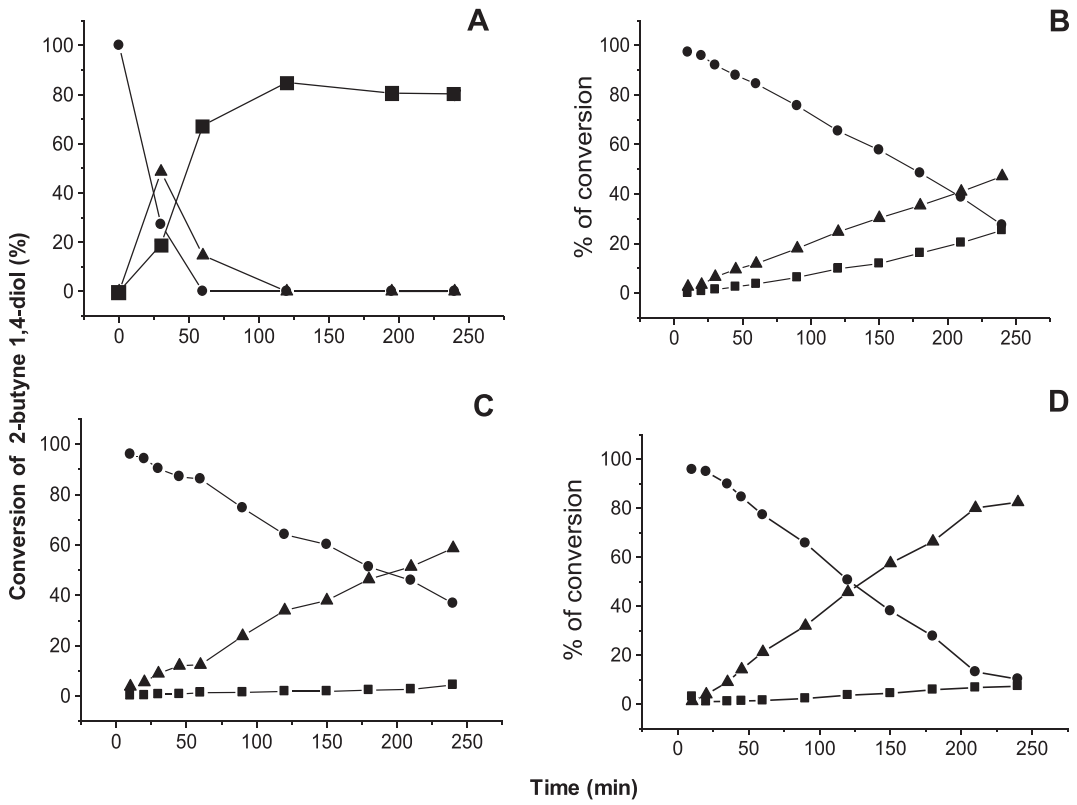

Fig. 5. Catalytic hydrogenation of 2-butyne-1,4-diol by commercial catalyst 5% Pd/alumina (A) and bio-Pd (20 wt%) on cells of *D. desulfuricans* (B) as in Fig. 1. C: conversion by 5 wt% bio-Pd (heat-processed) as in Fig. 2. D: conversion by 20 wt% bio-Pd (heat-processed). ●: 2-butyne-1,4-diol starting material and ▲: 2-butene-1,4-diol and ■: butane-1,4-diol. Note that carbon accounts for approximately 20% of biomass and hence catalyst was introduced at a constant mol% of Pd after estimation of the Pd content of the heat-treated carbonised biomaterial (see Experimental).

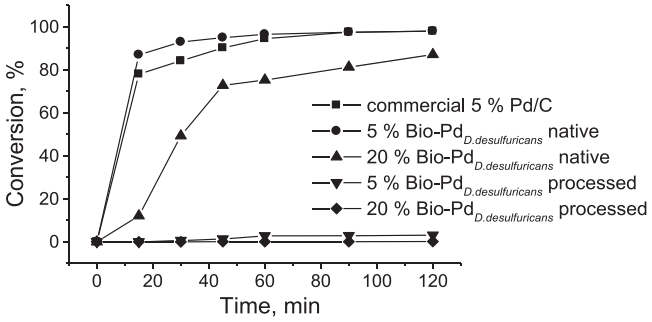

Fig. 6. Heck reaction profiles of iodobenzene and ethylacrylate over different catalysts (reaction by method 1). ■: Commercial 5% Pd/C catalyst. ▲: 20 wt% bio-Pd, native cells. ◆: 20 wt% bio-Pd, heat processed cells. ●: 5 wt% bio-Pd native cells. ▼: 5 wt% bio-Pd, heat processed cells.

the *D. desulfuricans* bio-Pd catalyst has the opposite effect to that observed in the hydrogenation reaction. Hence, the potential for heat-processing as a method for catalyst improvement must be evaluated on a case by case basis. Two studies using the Heck synthesis for production of ethyl cinnamate were performed independently several years apart using separate preparations of bio-Pd on *D. desulfuricans* in two independent laboratories by two methods (Figs. 6, 7). Fig. 6 shows that the *D. desulfuricans* bio-Pd outperformed the commercial catalyst by ~10% and Fig. 7 shows that the increased conversion via bio-Pd in the second study was >25%. The superiority of the bio-Pd catalyst was also confirmed in the conversion of styrene to stilbene which gave a similar result (not shown). Hence, we conclude, as indicated in early work [4], that native unprocessed bio-Pd has potential as a Heck catalyst.

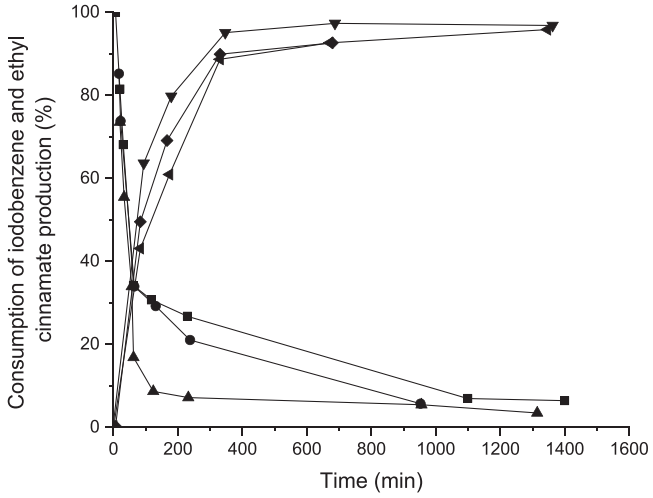

Fig. 7. Heck reaction profiles of iodobenzene and ethyl cinnamate using bio-Pd made by *D. desulfuricans* and CAS cells (method 2). Upper lines: Ethyl cinnamate formation (%). ◆: Commercial 5 wt% Pd/C catalyst.▼: 5 wt% Pd on *D. Desulfuricans*. ◀: 5 wt% Pd on CAS bacteria. Lower lines: Iodobenzene consumption (%).●: Commercial 5 wt% Pd/C catalyst. ▲: 5 wt% Pd on *D. desulfuricans* and ■: on CAS bacteria.

3.6. Comparison of Bio-Pd made on D. desulfuricans and waste sulfidogenic biomass from mine water remediation process

Apart from increased activity/selectivity of 5 wt% Pd on *D. desulfuricans* as compared to commercial chemical catalysts (above) the second criterion for catalyst acceptability is cheap and facile

production (see Introduction). Previous work established that a bio-Pd hydrogenation catalyst was made using waste *E. coli* bacteria [10] while more recent work [31] showed the application of a bio-Pd/Ru bimetallic, supported on a consortium of waste acidophilic sulfidogenic bacteria (CAS), in the conversion of 5-hydroxymethyl furfural to 2, 5-dimethyl furan. To establish the broader potential for using the bio-Pd of these 'second life' CAS bacteria, here in the Heck synthesis, reference cells of sulfidogenic *D. desulfuricans* (grown sulfidogenically and washed to remove H_2S and SO_4^{2-} carried over from the medium) and the CAS cells (taken from a continuous H_2S-producing reactor and similarly washed [31]) were compared in the Heck reaction in a commercial laboratory against 5 wt% Pd/C catalyst. The three catalysts showed a similar conversion rate and rate of ethyl cinnamate production (Fig. 7). The reaction slowed at ~ 70% conversion for the commercial and CAS-catalysts but proceeded to ~90% using 5 wt% bio-Pd on *D. desulfuricans* (Fig. 7). A similar yield of ethyl cinnamate was seen in each case (Fig. 7) which suggests the additional formation of other products by the *D. desulfuricans* bio-Pd (see Fig. 1) but this was not investigated further. It was concluded that a fully functional bio-Pd catalyst can be made using waste bacteria that gives a comparable performance to a commercial comparator.

4. Discussion

The two main findings of this study are that heat treatment of bio-Pd catalyst produced a superior hydrogenation catalyst and that bio-Pd made on waste bacteria produced a catalyst comparable to a commercial comparator in C-C bond formation. The CAS cells were not examined in the hydrogenation reaction; this, and evaluation of heat treatment of these, (to combine the two criteria of efficiency and economy) will be evaluated in follow-on work, along with more detailed structural studies of the catalysts, expanding upon the preliminary work shown in Supplementary Information. This would also entail a more detailed examination of interactions between metal catalytic NPs and amorphous carbon support derived from both bio- and activated carbon sources. A related study [40] combined high resolution electron microscopy and elemental mapping and confirmed that, as shown here, Pd-NPs are localized in the cell surface layers of *D. desulfuricans* with co-deposition of Pd with S and P [40] as found in outer membrane (S) and cell-associated lipopolysaccharides (P) (see NP-associated extrusions in Fig. 2c). The cells were washed and suspended in buffer with no added SO_4^{2-} but generation of H_2S via residual protein turnover by the cells cannot be excluded. Examination of the outermost surface of palladized cells of *D. desulfuricans* showed association with surface components by electron microscopy (elemental mapping [40]) while XPS confirmed (Fig. 3) the in situ reduction of Pd (II) on the cells of *D. desulfuricans* as changes in binding energy of unreduced Pd(II) solution (Fig. 3a) from 377.9 eV to 335.8 eV after reduction with atomic hydrogen onto the bacterial cell surfaces (Fig. 3b). This binding energy of ~335 eV is due to metal-metal interaction in Pd(0) whereas the binding energy at ~336.9–388 eV is due to Pd in + 2 valence state [48] as seen in the unreduced Pd(II) solution (Fig. 3a). The formation of a Pd-S bond with a binding energy of 163.4 eV suggests chemical interactions with bacterial cell surface groups like protein-thiols and sulfur-containing amino acids that have an ability to interact with incoming metals; Pd has high affinity for sulfur and coordinates to these ligands [49] as well as disulfides, and thioesters. The interaction between the Pd and the surface of the latter is weaker than for thiols and this can lead to advantages in some applications [50]. Low concentrations of sulfur and H_2S can prolong the life of a PGM catalyst [49], where the adsorption of sulfur on the catalyst surface can promote activity and, importantly, selectivity [51,52] as was seen here using the *D. desulfuricans* hydrogenation catalyst. Crudden et al. [53] pointed out that, while sulfur/sulfide is usually regarded as a catalyst poison (above), there are many examples to the contrary (see [53] for discussion) and these authors found (in the Mizoroki-Heck reaction), using thiol-modified support, an optimal ratio of S:P of between 2:1 and 4:1, with lower ratios promoting agglomeration [53].

The methods of examination of palladized cells used in this study are not necessarily complementary since XRD informs only about the crystalline components of the bulk sample while elemental mapping [40] co-locates elements spatially at individual single cell level, whereas XPS interrogates only the outermost ~10 nm of the cells in the bulk population but provides information on metal speciation in this region. The Pd-NPs are predominantly surface-localized: Fig. 2) and hence catalysis would occur mainly at the surface of the native palladized bacteria. The heat treatment promotes a reorganization of the material into Pd supported on large carbon spheres with Pd located at their surfaces (Fig. 4); heat treatment is also known to promote evolution of sulfided Pd (by loss of sulfur) into sulfur-lean phases such as Pd_4S, a known product of the heat processing of palladium sulfides [47]. Sulfided palladium species are well known as excellent selective catalysts for alkyne hydrogenation [47,54]. A previous study [47] used temperatures of up to 350 °C (i.e. below that used in the current work), reporting XRD peaks at 2-theta values which corresponded to the unidentified peaks shown in Supplementary Information Fig. S1 (dashed lines) which may be attributed to Pd_4S evolving from PdS as the temperature increased. Attempts to identify sulfur in the heat-treated biomaterial by EDX were equivocal due to the overlapping X-ray emissions of Pd and S (Fig. 4f); precise identification of the heat treated biomaterial awaits application of more advanced characterization methods such as proton induced X-ray emission and via synchtrotron radiation (i.e. excitation at higher energies in order to eject inner shell as well as outer shell electrons), enabling greater sensitivity as well as elemental differentiation and structural information. However, highly sensitive synchtrotron-mediated scanning X-ray mapping proved impossible to apply to bio-nanoparticles due to the low spatial resolution obtained (example data were shown in Supplementary Information to ref [31]).

With respect to hydrogenation, the factors impacting on product distribution for alkyne hydrogenation are wide-ranging and complex. Selectivity to partially-hydrogenated alkene products during the reduction of alkynes is known to be affected by pH [17,18] and the morphology of the catalyst particles, with higher coordination-number, extended terraces showing superior selectivity to internal *cis*-alkenes than more open surfaces [55,56]. In addition to the (111) and (200) facets, well-reported in bio-Pd on native cells, heat treated material also reveals (220), (222) and (311) facets, and hence likely crystal rearrangements (Supplementary Information Fig. S1). Since sublimation of Pd during heat treatment under vacuum was evidenced by the formation of black Pd deposits on the foil above the sample (I. Mikheenko, unpublished) this indicates physical rearrangements of Pd atoms during formation of the heat-treated material. Future studies would aim to identify the nature of such rearrangements, which is outside the scope of the current study.

The concentration of palladium hydrides (and indeed carbides), as may occur in the heat processed material (e.g. derived from membrane components: below), also affects hydrogenation selectivity. Subsurface hydrogen is more reactive for hydrogenation than surface hydrogen [57] while, at low pressures of H_2, palladium nanoparticles absorb more hydrogen than bulk palladium [58], leading to reduced alkene selectivity. Conversely, the agglomeration of the heat-treated NPs into larger particles would tend to reduce the hydrogen adsorption and hence be expected to enhance selectivity (which may also be the case with the agglomerated bio-Pds at 20 wt% loading of bio-Pd). Palladium carbide phases form under typical hydrogenation conditions and the C competes with H for lattice sites within the Pd ([59] and citations therein). However, the incorporation of C into the Pd lattice would also improve the rate of alkyne hydrogenation [60,61] and palladium carbide may also be the active phase for selective hydrogenations of some alkynes [62,63]. The presence of carbonaceous species on the surface of Pd particles also favours formation and replenishment of subsurface H, which is known to be required for olefin hydrogenation [64,65] which

would lower selectivity to partial-hydrogenation products from alkyne feedstocks. In addition, bio-Pd is an effective catalyst for the 'cracking' of bio-oils [66] and, due to the intimate association between bio-Pd and outer membrane lipids, carbide formation might be anticipated from these (below). Clearly further study of the structure of the bio-derived materials is required to gain further insight into the reaction mechanism.

A recent study [67] has gained further insight into the selective hydrogenation of propyne over a Pd-black model catalyst, comparing surface and subsurface chemistry in terms of Pd carbide and hydride species. This used *operando* XRD and XPS under reaction conditions at room temperature to confirm a role of PdC_x species formed by alkyne decomposition and carbon diffusion into the Pd lattice. In the case of the heat-treated biomaterial (which would benefit from a similar examination) it is likely that palladium carbides would be formed prior to the hydrogenation reaction, during Pd-catalyzed decomposition of, for example hydrocarbon membrane components that are seen to be associated with the Pd-NPs in Fig. 2c. Velasco- Vélez et al. [67] noted that carbide is difficult to assess based on XRD measurements in a system that contains palladium hydride, and hence the non-Pd peaks in Fig. S1 canot be assigned with certainty. The possibility to use NMR to examine noble metal nanoparticles has been reviewed [68]. This was achieved in the case of ^{105}Pd [69], where a range of Pd preparations was compared with the heat treated bio-Pd (Supplementary Information Fig. S3). Pd/C was not reported in [69] but the spectrum for this was similar to PVP-stabilized Pd [70]. The Knight shift (ppm) was largely nanoparticle size-independent (regardless of particle sizes in the nm to micron range) and the full width half maximum (FWHM, KHz) [69,70] was narrow in the case of Pd sponge and Pd black (respectively 13 ± 1 and 16 ± 1) while for Pd/C and PVP-stabilized Pd it was 80 ± 10 in each case, with a broad resonance shifted to higher frequencies [69,70] attributed to a deviation from the cubic Pd metal structure; ^{105}Pd NMR is sensitive to very small structural deviations from the nominal cubic struture. In contrast heat-treated bio-Pd showed a FWHM of 55 ± 15 [69] (Supplementary Information Fig. S3). The size of heat-treated bio-Pd particles was given as 2–1100 nm in the published work [69] as estimated by TEM and this reflects (but was not noted in [69]) the large size heterogeneity (Fig. 4e). Unlike the broad resonances of the PVP-stabilized Pd and Pd/C [69,70] the resonance of heat treated bio-Pd can be delineated into three clear Knight shifts (Supplementary Information Fig. S3) that were not discussed in the published work [69] and which, we suggest, may reflect the heterogeneity in structure of three sub-populations of the heat treated bio-Pd samples (micron sized particles and small NPs (Fig. 4e; Supplementary Information Fig. S3) which should not affect the Knight shift on the basis of size alone (see above and Supplementary Information Fig. S3). Such heterogeneity was not apparent in Pd/C [70] which suggests a factor(s) of the biomatrix that contributes to the material composition(s) and structure(s) as it evolves under heat treatment. Since hydrocarbon from membrane (lipid) materials is likely to be 'cracked' catalytically by the bio-Pd during evolution during heat treatment (above) [66] it is likely that the material contains resulting Pd-carbide and Pd-hydride components in addition to sulfided Pd (see above). Binuclear solid state NMR was achieved using ^{105}Pd and ^{1}H [70] and, given that decomposition of (e.g.) hydrocarbons over metallic catalysts is a standard method to produce carbon nanostructures (carbon nanotubes and other carbon-60 structures) bearing catalytic NPs, an examination of the heat treated biomaterial using ^{105}Pd together with ^{13}C NMR would be warranted in future studies to clarify the carbon speciation. Raman spectroscopy confirmed changes in the level of disorder and amorphous nature of the carbon in the sample post heat-treatment (Supplementary Information Fig. S4). A qualitative study in related work (Supplementary Information Fig. S5) shows small structures between the Pd particles (produced in this case at 700 °C and at atmospheric pressure under N_2) that could indicate the presence of carbon nanotubes but no conclusions can be drawn without further 'interrogation' of the carbon components following from preliminary work shown in Fig S5. Since Pd NPs supported on carbon nanotubes are now well established as catalysts (e.g. [71]), we suggest that the biomaterial may be a (bio)mimetic of such nanomaterials, sourcing carbon (and hydrogen) from the decomposition of, for example, hydrocarbon membrane components. Numerous reports exist of catalysts comprising Pd NPs supported on (e.g.) carbon nanotubes, for example Cano et al. [71] reported a Pd-catalyst made by this approach which showed good activity in both hydrogenation and C-C bond formation. However, since heat processing of bio-Pd gave material with no activity in the Heck synthesis this might argue against the formation of such carbon nanostructured material. Hence, further studies are required using carbon analysis methods, such as ^{13}C NMR, binuclear carbon and palladium NMR and also Raman spectroscopy; a preliminary analysis by the latter method had confirmed changes in the carbon of the material on heating (Supplementary Information Fig. S5).

We suggest that the high hydrogenation activity of the heat-processed material compared to Pd-NPs on native cells is likely to be attributable to the formation/evolution of palladium carbides (incorporation of carbon into the crystal lattice), possible carbon nanostructures forming in situ (Supplementary Information Fig. S5) and also 'sulfided' Pd, the latter evolving from PdS during heat treatment into PdS_4 [47,72]. Recent work by Albani et al. [72] suggests that S-enhanced catalyst contains selective ensembles comprising a nanostructured Pd_3S phase. The use of synchrotron-based methods would aim to further characterize the active components of native and heat-treated bio-Pd in sulfidogenic bacteria.

Regardless of the precise composition of the nanomaterial and its consequent effect on hydrogenation, the first conclusion of this study is that heat-processing of bio-Pd of *D. desulfuricans* produces a better catalyst than the commercial comparator with respect to selectivity, thus fulfilling criterion 1, in addition to the non-quantified environmental benefits (see Introduction). Towards criterion 2 (economy of catalyst production) the use of bio-Pd biorefined from metallic wastes was not evaluated in this current study; this was well-established previously with respect to hydrogenation of 2-pentyne and also soybean oil [3,73,74] as well as in upgrading reactions of both heavy fossil oil and pyrolysis oil sourced from wood and algal biomasses [3,5,66].

Looking towards green synthesis of higher value and 'niche' compounds, heat processed bio-Pd had no catalytic activity in C-C formation in the Heck reaction after heat treatment (Fig. 5). Hence, further studies on this reaction used native bio-Pd material with the goal of economy of production via up-valorization of bio-waste.

Heck reactions, and other classical C-C cross-coupling reactions, are conducted under homogeneous reaction conditions with soluble Pd-species supported in solution by complex ligand architectures, typically bespoke phosphine ligands amongst other possibilities (e.g. amines, sulfides, thiols) to tune the reactivity [23]. However, Heck reactions have also been successfully catalyzed by simple non-ligated Pd sources (e.g. $Pd(OAc_2)$) and heterogeneous solid-supported catalysts such as Pd/C which is a very commonly employed catalyst as it acts as a reservoir of soluble Pd which forms the actual catalytic species [23]. Later work confirmed that reactions proceed via Pd that has leached from the surface (see [53] for references). This has been possible at very low Pd levels, especially with reactive coupling partners such as aryl iodides as used here. The soluble Pd (the actual catalytic species, arising from Pd/C which acts as 'reservoir of soluble Pd [75]) forms, with aryl halide, a soluble aryl-Pd species and, when this substrate is depleted (i.e. at completion of the reaction), the Pd has no soluble supporting ligand and it redeposits on the support [75–77], which is essential for the removal of residual Pd from the solution (see earlier).

In addition to the detection of Pd(II) species in bio-Pd using XPS (see earlier) and the possible existence of an intermediate form of Pd (possibly Pd(I) [44]) migration of resolubilized, mobile Pd(II) was noted in an unrelated study [78]. Here, the formation of a bio-Pd/Au bimetallic was attributed to the galvanic reduction of Au(III) by bio-Pd(0), the resulting neo-Pd(II) species migrating to be re-reduced as Pd(0) at a 'shell' location [78]. Given that electronic exchanges also occur

between Pd atoms and supporting carbon components (specifically 'quenching' of carbon free radicals by single electrons from Pd [27]) it seems likely that a soluble species of Pd forms in situ, (i.e. NP 'turnover') with neo-Pd(I)/Pd(II) being 'competed for' by a cellular ligand taking over this functionality of aryl halide – i.e. a biomimetic system. Atom-scale elemental mapping with respect to cellular bio-Pd/Au NPs has indicated the possibility of a 'cloud' of 'orphan' Pd atoms (Supplementary Information Fig. S6). However, their 'local' mobility (and availability) cannot be examined by current methods in the biomatrix since X-ray imaging of fully hydrated cells in situ falls far short of the resolution required to follow single atom migrations (see example data in Supplementary Information shown in [31]).

Ther is ongoing debate of the role of inorganic Pd nanoparticles which are known to be generated under homogeneous reaction conditions [79,80]. It is not entirely clear whether the Pd nanoparticles formed in these reactions simply act as a reservoir of 'inert' Pd, or have a catalytic role, and if so, what. The size of such inorganic Pd nanoparticles may be key to their role and activity in such reactions, with smaller ones being highly active, and larger ones being less so or even inert. Large particles agglomerate and fall out of solution as "palladium black", with the Pd presumably no longer in the catalytic cycle (which occurs at the end of all cross-coupling reactions when the materials for the productive reaction have been consumed and other materials to stabilize/ligate Pd (e.g. aryl halide)) are no longer available. However, there is probably a strong dependence from phosphorus-ligands (phosphines are typically used commercially), on the result of the reaction. In the current case that function may be substituted by membrane phospholipids since metal-phosphate crosslinking of these polymers was shown [81] and co-localization of Pd and P was reported previously [36,40]. More specifically, ^{31}P NMR showed binding of Cd(II) to phosphate groups of the lipid A component of the lipopolysaccharide component of cell surface polymers, providing the crosslinking function [81]; this can be visualized by electron microscopy (Supplementary Information Fig. 7) and can be taken as a 'positive control' since electron microscopy of the CAS culture showed no extracellular metal (see earlier). Further studies might anticipate binuclear ^{105}Pd and ^{31}P NMR, and ^{105}Pd and ^{13}C NMR but the low sensitivity (compared to protons) would require long data acquisition times, this limitation precluding dynamic measurements.

In this study, comparable results were obtained with a 5% loading of both Pd/C and native bio-Pd (Fig. 6). Some leaching of Pd into solution must be assumed in the case of Pd/C, and this seems equally likely in the case of bio-Pd, especially given the detection of 'orphan' atoms around metallic nanoparticles in the biomass (above) which comprises mostly water and hydrated polymers interfacing with hydrophobic components. In a 'chemical' system leached Pd should end up in the product, be lost on the reactor wall, or most likely, be re-absorbed back onto the surface support from which it came (see above), since this provides a strong surface interaction, known to occur with sulfide-Pd [53]. Although soluble Pd species were not detected in the mixture post reaction following removal of the bio-Pd [7] determining the levels of Pd in the product or the reaction solution would be difficult at the very low levels probably present and, as noted, this particular reaction pairing can proceed at very low Pd levels. As noted above, the biomimetic system we report here follows an early report whereby thiol-modified mesoporous silica was used as a Pd scavenger and catalyst support. These authors [53] reported more than 99.9% removal of Pd from a 1 ppm solution of Pd(II). The material was catalytically active in the Mizoroki-Heck reaction; after completion of the reaction the residual soluble Pd was 0.2 ppm. We suggest that bio-Pd is a biomimetic of this functional nanomaterial.

The total loss of activity in the case of the two heat-treated bio-Pd NP samples (Fig. 6) compared to the native bio-Pd provides an unequivocal contrast to that of heat treatment upon bio-Pd in the hydrogenation reaction, which is surface mediated, in combination with absorbed H_2 gas (see earlier/later discussion). In this system, the Heck reaction is not mediated by classical Pd-ligating ligands, and so, apart from extruded bio-material (e.g. putative phospholipid fragments: Fig. 2c: above) the Pd would not be supported in solution beyond the potentiality of the solvent and the reaction materials themselves. Soluble non-ligated Pd nanoparticles, even down to single atoms (above), potentially may be dominant in this reaction mechanism. If so, heat treatment of both 5 and 20 wt% loadings of bio-Pd may have altered/affected/reduced the availability/population of available smaller nanoparticles, probably by agglomeration into the large structures shown in Fig. 4, thus making them unable to release soluble Pd species into solution; Fig. 4d shows that the Pd particles are now predominantly in the μm range. This may also suggest why the native 20 wt% bio-Pd was less active than the 5 wt % bio-Pd, (although it eventually approached a similar conversion) if the process of a heavier Pd loading on the cells has resulted in fewer small nanoparticles. However, as shown in Figs. 2c and 2d, larger NPs are actually agglomerations and consolidations of small ones that provide a convoluted 'surface' and high surface area and a true representation may not be achieved until a method of increasing NP homogeneity (i.e. a better cellular dispersion of very small NPs) is achieved. The use of microwave-injury to the cells before and during fabrication of bio-Pd has been shown to achieve this effect, with resulting enhancement of catalytic activity by 2–3 fold [82].

A comparison of bio-Pd supported by *D. desulfuricans* and the CAS cells showed that the *D. desulfuricans* biomaterial gave a better conversion to ethyl cinnamate, i.e. the reaction proceeded further towards completion. Hence, since the yield of ethyl cinnamate was comparable (Fig. 6), this would imply the presence of other by-products in the bio-Pd *D. desulfuricans* reaction which was not investigated further. The bio-Pd of the CAS would be the catalyst of choice as, in addition to being sourced from a waste, its performance (and product yield) was comparable to the commercial equivalent. The Heck reaction (reviewed in (e.g.) [21,83–85]) is thought to be mediated in heterogeneous catalysts by soluble Pd(II) species derived from the solid phase (above), (and a Pd (II)/Pd(IV) cycle), and not via the surface of bulk Pd(0). The primary mode of leaching was suggested to be via the oxidative addition of aryl iodide to the Pd(0) surface (above), releasing soluble Pd(II) species into solution and this mechanism, now accepted (overviewed and discussed in [23]) would be mimicked via the local complexation of Pd(II) onto bioligands (above) but this was not investigated in the case of CAS cells.

'Sulfided' Pd, as noted with *D. desulfuricans*, was identified conclusively on the CAS bacteria by XPS and was confirmed via scanning X-ray microscopy using synchtrotron radiation (Supplementary Information in ref [31]). Following extensive washing of the CAS cells a strong sulfide odor was noted that was absent from *D. desulfuricans*. The relative amounts of sulfided Pd (as compared to Pd(0)) in each case were not determined but, given that in a mixed bacterial population, both sulfide cycling and storage of readily mobilized polysulfides was likely (see [31]) an endogenous source of mobile sulfide would be brought into the bio-Pd synthesis by the CAS cells (which would be absent from the *D. desulfuricans* monoculture) and contribute more sulfide, thus bringing the S:Pd ratio towards the 2:1–4:1 that was concluded to be optimal by Crudden et al. [53] using thiol ligands as support for palladium species in Heck coupling reactions (reviewed in [23]). This comprehensive review [23] notes that examination of the thiol-supported precatalysts by X-ray absorption spectroscopy (both EXAFS and XANES) showed that Pd comprised Pd(II) species bound to two or more thiol groups. It was suggested that the thiols may prevent large amounts of Pd from desorbing and then aggregating as Pd(0) clusters. However, it is generally accepted that various solid catalysts, including thiol-functionalized silicas, all leached active, soluble Pd species in the Heck coupling of n-butylacrylate and iodobenzene, with no conclusive evidence for catalysis by any solid species.

Other studies have also noted the utility of using thiol-functionalized support for Heck catalyst production, among these thiol-functionalized mesoporous silica [53] and thiol functionalized chitosan (a biopolymer derived from chitin which is produced in large quantities

from shellfish wastes as well as fungal fermentations [86]) and, indeed, thiol derived from cysteine [87] as would occur during protein turnover in resting cells. In the CAS, storage of intracellular polysulfides in inclusion bodies, and mobilization as H_2S was suggested to allow continued formation of H_2S during formation of Pd NPs in the absence of added sulfate/sulfide [31]. It is likely that the CAS waste bacteria are fortuitously producing/storing the material in advance, that they will 'need' in 'second life' which has major implications for economy and sustainability. On the other hand, formation of palladium polysulfide per se by CAS cells (i.e. without mobilization of polysulfide into H_2S) is not precluded. Palladium polysulfide has been described [88,89] whereby Pd atoms are linked via S chains in an array with no discrete PdS groups; the structure was reported to differ from other polysulfide complexes, comprising non-chelated S_6 chains linking planar Pd(II) ions. A recent review [90] notes the ubiquity of polysulfides in the biosphere and geosphere and also a possible geochemical role for them in the transport/mobilization of Au and Pt (noble metals) in the geosphere. Other work [91] using in situ X-ray absorption spectroscopy and theoretical calculations established that S_3 contributes to gold solubility in aqueous solutions at high temperatures and pressures, with $Au(SH)S_3$ identified as the most stable complex. The same mechanism(s) was suggested to apply to platinum group metals [91], while (bio) geochemical studies have shown a role for microbial processes in the mobility and deposition of both Au and platinum group metals in the geosphere (see [92] and references therein); no detailed explanations describe the underlying mechanisms but sulfur ligands (e.g. thiosulfate) have been implicated in increasing the solubility of these noble metals and in re-formation of secondary metallic deposits [92]. We suggest that a similar mechanism is at play here, with the Heck catalytic cycle 'intervening' in a natural process of Pd(0)/Pd(II) turnover. In this sense the CAS bacteria are a natural development from biogeochemical processes and future studies would aim to confirm this as a natural biomimetic system: learning from nature.

Haradem et al. [88] highlighted that the molecular structure of palladium polysulfides precludes working with these compounds in solution, while Steudal and Chivers [90] reiterated that work with polysulfides in (hydrated) biological samples is challenging. We suggest as a working hypothesis that at least part of the catalytically active Pd in the CAS bacteria may be attributable to PdS derived from mobilizable [93] polysulfide (e.g. via H_2S) or to Pd-polysulfide itself (i.e. Pd(II) obtained from it: see earlier).

The participation of polysulfide storage materials in fabrication of active Pd catalyst would be difficult to prove, and is outside the scope of the current work although the circumstantial evidences point to this possibility. A key factor is that the CAS population has been evolved from a natural inoculum and is a mixture of various bacterial types. With regards to the stability of the population of the CAS culture, this has been established over several years with respect to the proportions of the sulfur oxidizing and sulfate-reducing bacterial components (D.B. Johnson and co-workers, unpublished data) that would combine to bring a mobilizable form of sulfide [31,91] into the resting cells used for Pd-NP manufacture.

More work is needed to elucidate the active species of (sulfided and non-sulfided) Pd-NPs made by the *D. desulfuricans* and CAS cells, though we conclude that for hydrogenation heat treated bio-Pd is particularly useful (see above) whereas for the Heck reaction an economic option is provided by the use of the CAS waste bacteria. Notably, these also gave a superior catalyst (as bimetallic bio-Pd/Ru) in up-conversion of 5-hydroxymethyl furfural to 2,5-dimethyl furan [31]. Hence, this present study fulfilled both key criteria for new catalyst adoption as well as entering unknown territory regarding possible roles of palladium polysulfides and carbides in addition to Pd(0). Studies will now seek to delineate the roles of the palladium and/or sulfur components and optimize the pathway(s) of sulfidogenesis in resting CAS cells in order to produce 'tailored' catalysts and to explore further the scope of bio-Pd (and bimetallics) on CAS bacteria across a suite of industrially relevant reactions. The present study did not evaluate the use of heat-treated CAS bacteria (potentially fulfilling both criteria) but this will form the basis of future work, along with the role of sulfided Pd species (above).

Three additional factors should also be noted. First, no attempt was made at optimization of reaction conditions in this study (optimal conditions may differ for the 'classical' and biogenic catalysts) in order to compare 'like for like'. Second, commercial catalysts have been extensively developed over many years, reflecting major investments by large industries, whereas this is the first study of its kind (focusing on meeting established criteria) using 'green' biogenic catalysts with no attempt at process optimization; to show comparability between the disparate catalysts in this first study is a major advance, while preliminary analyses of the biomaterials provides indications of how they may differ from classically-made catalysts ('cause and effect'). Third, waste up-valorization is seen as key to development of the circular economy [94,95]. as well as in mitigating the carbon burden of synthesis of 'for purpose' primary materials.

CRediT authorship contribution statement

All authors contributed to this submission**. I. Mikheenko**, **J.A. Bennett** and **J. B. Omajali** carried out experimental work at University of Birmingham (catalyst preparation and testing), **M.Walker** did XPS work at University of Warwick, **D. Johnson** supervised work at Bangor University (production of second life biomass), carried out by **B. M. Grail**, **David Wong-Pascua** carried out catalytic testing in reference commercial laboratory overseen by **J. D. Moseley**, **L. E. Macaskie** oversaw/coordinated work at U. of Birmingham, secured funds to support the work and authored the manuscript, All authors commented on and approved the manuscript.

Declaration of Competing Interest

The authors declare that they have no known competing financial interests or personal relationships that could have appeared to influence the work reported in this paper.

Acknowledgements

This work was supported by the Biotechnology and Biosciences Research Council, UK (Grant no. BB/C516128/1), a Biotechnology and Biosciences Research Council, UK Pathfinder Award and Natural Environment Research Council, UK (Grant No NE/L014076/1) to LEM. The authors wish to thank Dr J. Gomez-Bolivar for useful discussions. They also declare no conflicts of interest.

Appendix A. Supporting information

Supplementary data associated with this article can be found in the online version at doi:10.1016/j.apcatb.2021.121059.

References

[1] L.E. Macaskie, I.P. Mikheenko, J.B. Omajali, A.J. Stephen, J. Wood, Metallic bionanocatalysts: potential applications as green catalysts and energy materials, Microbial, Microbial Biotechnol. 10 (2017) 1171–1180, https://doi.org/10.1111/1751-7915.12801.

[2] S. De Corte, T. Hennebel, B. De Guisseme, W. Verstraete, N. Boon, Bio-palladium: from metal recovery to catalytic applications, Microbial Biotechnol. 5 (2012) 5–17, https://doi.org/10.1111/j.1751-7915.2011.00265.x.

[3] A.J. Murray, I.P. Mikheenko, K. Deplanche, J.B. Omajali, J. Gomez-Bolivar, M. Merroun, L.E. Macaskie, Chapter 9 in resource recovery from waste, in: L. E. Macaskie, D.J. Sapsford, W.M. Mayes (Eds.), Towards a Circular Economy, Royal Society of Chemistry, London, 2019, pp. 213–243. ISBN 978-1-78801-381-9.

[4] K. Deplanche, J.A. Bennett, I.P. Mikheenko, J.B. Omajali, A.S. Wells, R. E. Meadows, J. Wood, L.E. Macaskie, Catalytic activity of biomass-supported Pd nanoparticles: Influence of the biological component in catalytic efficacy and potential application in 'green' synthesis of fine chemicals and pharmaceuticals,

Appl. Catal. B Environ. 147 (2014) 651–665, https://doi.org/10.1016/j.apcatb.2013.09.045.
[5] S.A. Archer, A.J. Murray, J.B. Omajali, M. Paterson-Beedle, B.K. Sharma, J. Wood, L.E. Macaskie, in: L.E. Macaskie, D.J. Sapsford, W.M. Mayes (Eds.), Chapter 13 in Resource Recovery from Waste: Towards a Circular Economy, Royal Society of Chemistry, London, 2019, pp. 315–342. ISBN 978-1-78801-381-9.
[6] A.J. Mabbett, D. Sanyahumbi, P. Yong, L.E. Macaskie, Biorecovered precious metals from industrial wastes: single-step conversion of a mixed metal liquid waste to a bioinorganic catalyst with environmental application, Environ. Sci. Technol. 40 (2006) 1015–1021, https://doi.org/10.1021/es0509836.
[7] J.A. Bennett, I.P. Mikheenko, K. Deplanche, I. Shannon, J. Wood, L.E. Macaskie, Nanoparticles of palladium supported on bacterial biomass: new re-usable heterogeneous catalyst with comparable activity to homogeneous colloidal Pd in the Heck reaction, Appl. Catal. B Environ. 140–141 (2013) 700–707, https://doi.org/10.1016/j.apcatb.2013.04.022.
[8] D. Beauregard, P. Yong, M.L. Johns, L.E. Macaskie, Using non-invasive magnetic resonance imaging (MRI) to assess the reduction of Cr(VI) using a biofilm–palladium catalyst, Biotechnol. Bioeng. 107 (2010) 11–20.
[9] P. Yong, W. Liu, Z. Zhang, D. Beauregard, M.L. Johns, L.E. Macaskie, One step bioconversion of waste precious metals into *Serratia* biofilm-immobilised catalyst for Cr(VI) reduction, Biotechnol. Lett. 37 (2015) 2181–2191, https://doi.org/10.1002/bit.22791.
[10] J. Zhu, J. Wood, K. Deplanche, L.E. Macaskie, Selective hydrogenation using palladium bioinorganic catalyst, Appl. Catal. B Environ. 199 (2016) 108–122, https://doi.org/10.1016/j.apcatb.2016.05.060.
[11] H. Gräfje, W. Körnig, H.M. Weitz, W. Reiß, G. Steffan, H. Diehl, H. Bosche, K. Schneider, H. Kieczka, Butanediols, butenediol, and butynediol. in: Ullmann's Encyclopedia of Industrial Chemistry, Wiley-VCH, Weinheim, 2000, https://doi.org/10.1002/14356007.a04_455.
[12] R. del Rosso, C. Mazzocchia, P. Gronchi, P. Centola, Influence of some reaction parameters in the hydrogenation of 1,4-butynediol to 1,4-butanediol on a ruthenium based catalyst, Appl. Catal. 9 (1984) 269–277, https://doi.org/10.1016/0166-9834(84)80071-8.
[13] I.T. Duncanson, I.W. Sutherland, B. Cullen, S.D. Jackson, D. Lennon, The hydrogenation of 2-butyne-1,4-diol over a carbon-supported palladium catalyst, Catal. Lett. 103 (2005) 195–199, https://doi.org/10.1007/s10562-005-7154-6.
[14] J.M. Winterbottom, H. Marwan, J. Viladevall, S. Sharma, S. Raymahasay, Selective catalytic hydrogenation of 2-butyne-1,4-diol to cis-2-butene-1,4-diol in mass transfer efficient slurry reactors, Stud. Surf. Sci. Catal. 108 (1997) 59–69, https://doi.org/10.1016/S0167-2991(97)80888-9.
[15] A. Knapik, A. Drelinkiewicz, A. Waksmundzka-Gora, A. Bukowska, W. Bukowski, J. Noworo, Hydrogenation of 2-butyn-1,4-diol in the presence of functional crosslinked resin supported Pd catalyst. the role of polymer properties in activity/selectivity pattern, Catal. Lett. 122 (2008) 155–166, https://doi.org/10.1007/s10562-007-9362-8.
[16] M.G. Musolino, C.M.S. Cutrupi, A. Donato, D. Pietropaolo, R. Pietropaolo, Liquid phase hydrogenation of 2-butyne-1,4-diol and 2-butene-1,4-diol isomers over Pd catalysts: roles of solvent, support and proton on activity and products distribution, J. Mol. Catal. A 195 (2003) 147–157, https://doi.org/10.1016/S1381-1169(02)00547-2.
[17] M.M. Telkar, C.V. Rode, V.H. Rane, R. Jaganathan, R.V. Chaudhari, Selective hydrogenation of 2-butyne-1,4-diol to 2-butene-1,4-diol: roles of ammonia, catalyst pretreatment and kinetic studies, Appl. Catal. A 216 (2001) 13–22, https://doi.org/10.1016/S0926-860X(01)00547-6.
[18] L. Kiwi-Minsker, E. Joannet, A. Renken, Solvent-free selective hydrogenation of 2-butyne-1,4-diol over structured palladium catalyst, Ind. Eng. Chem. Res. 44 (2005) 6148–6153, https://doi.org/10.1021/ie049107b.
[19] R.F. Heck, in: B.M. Trost, I. Fleming (Eds.), Comprehensive Organic Synthesis, 4, Pergamon Press, Oxford, 1991 ch. 4.3.
[20] A. de Meijere, F.E. Meyer, Fine feathers make fine birds: the Heck reaction in modern garb, Angew. Chem. Int. Ed. 33 (1995) 2379–2411, https://doi.org/10.1002/anie.199423791.
[21] M. Oestreich (Ed.), The Mizoroki-Heck Reaction, John Wiley & Sons, Chichester UK, 2009.
[22] L. Huang, Z. Wang, T.P. Ang, J. Tan, P.K. Wong, A novel SiO_2 supported Pd metal catalyst for the Heck reaction, Catal. Lett. 112 (2006) 219–226, https://doi.org/10.1007/s10562-006-0206-8.
[23] N.T.S. Phan, M. van der Sluys, C.W. Jones, On the nature of the active species in palladium catalyzed Mizoroki-Heck and Suzuki-Miyaura couplings – homogeneous or heterogeneous catalysis, a critical review, J. Adv. Syn. Catal. 348 (2006) 609–679, https://doi.org/10.1002/adsc.200505473.
[24] N.J. Creamer, I.P. Mikheenko, P. Yong, K. Deplanche, D. Sanyahumbi, J. Wood, K. Pollmann, M. Merroun, S. Selenska-Pobell, L.E. Macaskie, Novel supported Pd hydrogenation bionanocatalyst for hybrid homogeneous/heterogeneous catalysis, Catal. Today 128 (2007) 80–87, https://doi.org/10.1016/j.cattod.2007.04.014.
[25] Y. Ji, J. Surbhi, R. Davis, Investigation of Pd leaching from supported Pd catalysts during the Heck reaction, J. Phys. Chem. B 109 (2005) 17232–17238, https://doi.org/10.1021/jp052527.
[26] P. Yong, M. Paterson-Beedle, I.P. Mikheenko, L.E. Macaskie, From bio-mineralisation to fuel cells: biomanufacture of Pt and Pd nanocrystals for fuel cell electrode catalyst, Biotechnol. Lett. 29 (2007) 539–544, https://doi.org/10.1007/s10529-006-9283-4.
[27] R.P. Carvalho, P. Yong, I.P. Mikheenko, M. Paterson-Beedle, L.E. Macaskie, Electron paramagnetic resonance analysis of active bio-Pd-based electrode for fuel cells, Adv. Mat. Res. 71–73 (2009) 737–740, https://doi.org/10.4028/www.scientific.net/AMR.71-73.737.
[28] P. Yong, I.P. Mikheenko, K. Deplanche, M.D. Redwood, L.E. Macaskie, Biorefining of precious metals from wastes: an answer to manufacturing of cheap nanocatalysts for fuel cells and power generation via an integrated biorefinery? Biotechnol. Lett. 32 (2010) 1821–1828, https://doi.org/10.1007/s10529-010-0378-6.
[29] I.P. Mikheenko, M. Rousset, S. Dementin, L.E. Macaskie, Bioaccumulation of palladium by *Desulfovibrio fructosivorans* wild-type and hydrogenase-deficient strains, Appl. Environ. Microbiol. 19 (2008) 6144–6146, https://doi.org/10.1128/AEM.02538-07.
[30] K. Deplanche, I. Caldelari, I.P. Mikheenko, F. Sargent, L.E. Macaskie, Involvement of hydrogenases in the formation of highly catalytic Pd(0) nanoparticles by bioreduction of Pd(II) using *Escherichia coli* mutant strains, Microbiol 156 (2010) 2630–2640, https://doi.org/10.1099/mic.0.036681-0. ⟨https://doi⟩.
[31] I.P. Mikheenko, J. Gomez-Bolivar, M.L. Merroun, L.E. Macaskie, S. Sharma, M. Walker, R.A. Hand, B.M. Grail, D.B. Johnson, R.L. Orozco, Upconversion of cellulosic waste into a potential "drop in fuel" via novel catalyst generated using *Desulfovibrio desulfuricans* and a consortium of acidophilic sulfidogens, Front. Microbiol. 10 (2019), 970, https://doi.org/10.3389/fmicb.2019.00970.
[32] I. Sánchez-Andrea, A.J. Stams, S. Hedrich, I. Ñancucheo, D.B. Johnson, *Desulfosporosinus acididurans* sp. nov.: an acidophilic sulfate-reducing bacterium isolated from acidic sediments, Extremophiles 19 (2015) 39–47, https://doi.org/10.1007/s00792-014-0701-6.
[33] A.L. Santos, D.B. Johnson, The effects of temperature and pH on the kinetics of an acidophilic sulfidogenic bioreactor and indigenous microbial communities, Hydrometall 168 (2017) 116–120, https://doi.org/10.1016/j.hydromet.2016.07.018.
[34] . Charlot. Dosages Absorptiometriques des Elements Mineraux. Masson Ed. Paris, (1978).
[35] J.R. Lloyd, P. Yong, L.E. Macaskie, Enzymatic recovery of elemental palladium by using sulfate-reducing bacteria, Appl. Environ. Microbiol. 64 (1998) 4607–4609, https://doi.org/10.1128/AEM.64.11.4607-4609.1998.
[36] J.B.Omajali, Novel Bionanocatalysts for Green Chemistry Applications (Ph.D. thesis), University of Birmingham, UK, 2015.
[37] J.B. Omajali, I.P. Mikheenko, M.L. Merroun, J. Wood, L.E. Macaskie, Characterization of intracellular palladium nanoparticles synthesized by *Desulfovibrio desulfuricans* and *Bacillus benzeovorans*, J. Nanopart. Res. 17 (2015) 264, https://doi.org/10.1007/s11051-015-3067-5.
[38] M. Zieniewickz-Strzalka, S. Pikus, The study of palladium ions incorporation into the mesoporous ordered silicates, Appl. Surf. Sci. 261 (2012) 616–622, https://doi.org/10.1016/j.apsusc.2012.08.065.
[39] J.B. Omajali, A. Hart, M. Walker, J. Wood, L.E. Macaskie, In-situ catalytic upgrading of heavy oil using dispersed bionanoparticles supported on gram-positive and gram-negative bacteria, Appl. Catal. B Environ. 203 (2017) 807–819, https://doi.org/10.1016/j.apcatb.2016.10.074.
[40] J. Gomez-Bolivar, I.P. Mikheenko, M.L. Merroun, L.E. Macaskie, Characterization of palladium nanoparticles produced by healthy and microwave-injured cells of *Desulfovibrio desulfuricans* and *Escherichia coli*, Nanomaterials 9 (2019) 857–873, https://doi.org/10.3390/nano9060857.
[41] R. Priestley, A. Mansfield, J. Bye, K. Deplanche, A. Jorge, D. Brett, L.E. Macaskie, S. Sharma, Pd nanoparticles supported on reduced graphene–*E. coli* hybrid with enhanced crystallinity in bacterial biomass, RSC Adv. 5 (2015) 84093–84103, https://doi.org/10.1039/C5RA12552A.
[42] E.Torgeman, Biosynthesis of Gold and Palladium Nanoparticles via Bacteria (MSc thesis), University of Oslo, 2017.
[43] R. Koebnik, K.P. Locher, P. Van Gelder, Structure and function of bacterial outer membraneproteins: barrels in a nutshell, Mol. Microbiol. 37 (2000) 239–253, https://doi.org/10.1046/j.1365-2958.2000.01983.x.
[44] I. de Vargas, D.Sanyahumbi, M.A. Ashworth, C.M. Hardy, L.E. Macaskie, Use of X ray photoelectron spectroscopy to elucidatethe mechanism of palladium and platinum biosorption by Desulfovibriodesulfuricans biomass, In: S.T.L. Harrison, D. E. Rawlings, J. Petersen (Eds.), Proceedings of the Sixteenth International Symposium on Biohydrometallurgy Cape Town, South Africa 25– 29 September 2005, University of Cape Town, 605-616.
[45] K. Gotterbarm, N. Luckas, O. Hoefert, M.P.A. Lorenz, R. Streber, C. Papp, F. Vines, H.-P. Steinrueck, A. Goerling, Kinetics of the sulfur oxidation on palladium: a combined in situ X-ray photoelectron spectroscopy and density-functional study, J. Chem. Phys. 136 (2012), 094702, https://doi.org/10.1063/1.3687676.
[46] S. Li, A. Pasc, V. Fierro, A. Celzard, Hollow carbon spheres, synthesis and applications–a review, J. Mater. Chem. 4 (2016) 12686–12713, https://doi.org/10.1039/C6TA03802F.
[47] Y. Liu, A.J. McCue, J. Feng, S. Guan, D. Li, J.A. Anderson, Evolution of palladium sulfide phases during thermal treatments and consequences for acetylene hydrogenation, J. Catal. 364 (2018) 204–215, https://doi.org/10.1016/j.jcat.2018.05.018.
[48] M. Hasik, A. Bernasik, A. Drelinkiewicz, K. Kowalski, E. Wenda, J. Camra, XPS studies of nitrogen-containing conjugated polymers–palladium systems, Surf. Sci. 507–510 (2002) 916–921, https://doi.org/10.1016/S0039-6028(02)01372-9.
[49] J.K. Dunleavy, Sulfur as a catalyst poison, Platin. Met. Rev. 50 (2006) 110–111, https://doi.org/10.1595/147106706×111456.
[50] J. Cookson, The Preparation of palladium nanoparticles, Platin. Met. Rev. 56 (2012) 83–98, https://doi.org/10.1595/147106712×632415.
[51] A.J. McCue, J.A. Anderson, Sulfur as a catalyst promoter or selectivity modifier in heterogeneous catalysis, Catal. Sci. Technol. 4 (2014) 272–294, https://doi.org/10.1039/C3CY00754E.
[52] Y.J. Tong, Unconventional promoters of catalytic activity in electrocatalysis, Chem. Soc. Rev. 41 (2012) 8195–8209, https://doi.org/10.1039/C2CS35381D.

[53] C.M. Crudden, K. McEleney, S.L. MacQuarrie, A. Blanc, M. Sateesh, J.D. Webb, Modified mesoporous materials as Pd scavengers and catalyst supports, Pure Appl. Chem. 79 (2007) 247–260, https://doi.org/10.1351/pac200779020247.
[54] X. Zhao, L. Zhou, W. Zhang, B. Wu, G. Fu, N. Zheng, Thiol treatment creates selective palladium catalysts for semihydrogenation of internal alkynes, Chemistry 4 (2018) 1080–1091, https://doi.org/10.1016/j.chempr.2018.02.011.
[55] J.G. Ulan, W.F. Maier, D.A. Smith, Rational design of a heterogeneous palladium catalyst for the selective hydrogenation of alkynes, J. Org. Chem. 52 (1987) 3132–3142, https://doi.org/10.1021/jo00390a032.
[56] J.A. Bennett, G.A. Attard, K. Deplanche, M. Casedesus, S.E. Huxter, L.E. Macaskie, J. Wood, Improving selectivity in 2-butyne-1,4-diol hydrogenation using biogenic Pt catalysts, ACS Catal. 2 (2012) 504–511, https://doi.org/10.1021/cs200572z.
[57] A.D. Johnson, S.P. Daley, A. Utz, S. Ceyer, The chemistry of bulk hydrogen: reaction of hydrogen embedded in nickel with adsorbed CH_3, Science 257 (1992) 223–225, https://doi.org/10.1126/science.257.5067.223.
[58] M. Wilde, K. Fukutani, M. Naschitzki, H.J. Freund, Hydrogen absorption in oxide-supported palladium nanocrystals, Phys. Rev. B 77 (2008), 113412, https://doi.org/10.1103/PhysEvB.77.113412.
[59] A. Borodzinski, G.L. Bond, Selective hydrogenation of ethyne in ethene-rich streams on palladium catalysts. part 1. effect of changes to the catalyst during reaction, Catal. Rev. 48 (2006) 91–144, https://doi.org/10.1080/01614940500364909.
[60] A. Borodzinski, The effect of carburization of palladium catalysts on the hydrogenation of acetylene-ethylene mixtures, Pol. J. Chem. 72 (1998) 2455–2462.
[61] A. Borodzinski, The effect of carbonaceous deposits of alumina on hydrogenation of acetylene-ethylene mixture on Pd/Al_2O_3, Pol. J. Chem. 69 (1995) 111–117.
[62] D. Teschner, J. Borsodi, A. Wootsch, Z. Révay, M. Hävecker, A. Knop-Gericke, S. D. Jackson, R. Schlögl, The roles of subsurface carbon and hydrogen in palladium-catalyzed alkyne hydrogenation, Science 320 (2008) 86–89, https://doi.org/10.1126/science.1155200.
[63] D. Teschner, E. Vassm, M. Hävecker, S. Zafeiratos, P. Schnorch, H. Sauer, A. Knop-Gericke, R. Schlögl, M. Chamam, A. Wootsch, A.S. Canning, J.J. Gamman, S. D. Jackson, J. McGregor, L.F. Gladdenet, Alkyne hydrogenation over Pd catalysts: a new paradigm, J. Catal. 242 (2006) 26–37, https://doi.org/10.1016/j.jcat.2006.05.030.
[64] M. Wilde, K. Fukutani, W. Ludwig, B. Brandt, J.H. Fischer, S. Schauerman, H. J. Freund, Influence of carbon deposition on the hydrogen distribution in pd nanoparticles and their reactivity in olefin hydrogenation, Angew. Chem. Int. Ed. 47 (2008) 9289–9293, https://doi.org/10.1002/anie.200801923.
[65] D. Teschner, J. Barsodi, Z. Kis, l, Z. Szentniklos, Révay a. Knop-Gericke, R. Schög, D. Torres, P. Sautet, Role of hydrogen species in palladium-catalyzed alkyne hydrogenation, J. Phys. Chem. C 114 (2010) 2293–2299, https://doi.org/10.1021/jp9103799.
[66] B. Kunwar, S.D. Deilami, L.E. Macaskie, J. Wood, P. Biller, B.K. Sharma, Nanoparticles of Pd supported on bacterial biomass for hydroprocessing crude bio-oil, Fuel 209 (2017) 449–456, https://doi.org/10.1016/j.fuel.2017.08.007.
[67] J.J. Velasco- Vélez, D. Teschner, F. Girgsdies, M. Hävecker, V. Streibel, M. G. Willinger, J. Cao, M. Lamoth, E. Frei, R. Wang, A. Centeno, A. Zurutuza, S. Hofmann, R. Schlögl, A. Gericke, The role of adsorbed and subsurface carbon species for the selective alkyne hydrogenation over a Pd-black catalyst: an operando study of bulk and surface, Top. Catal. 61 (2018) 2052–2061, https://doi.org/10.1007/s11244-018-1071-6.
[68] L.E. Marbella, J.E. Millstone, NMR techniques for noble metal nanoparticles, Chem. Mater. (2015) 2782721–2782739, https://doi.org/10.1021/cm504809c.
[69] T.J.N. Hooper, T.A. Partridge, G.J. Rees, D.S. Keeble, N.A. Powell, M.E. Smith, I. P. Mikheenko, L.E. Macaskie, P.T. Bishop, J.V. Hanna, Direct solid state NMR observation of the ^{105}Pd nucleus in inorganic compounds and palladium metal systems, Phys. Chem. Chem. Phys. 20 (2018) 26734–26743, https://doi.org/10.1039/C8CP02594K.
[70] J.T.N. Hooper, Solid State Nuclear Magnetic Resonance on Quadrupolar Nuclei in Disordered Catalysis Based Materials (Ph.D. thesis), University of Warwick, UK, 2017.
[71] M. Cano, A. Benito, W.K. Maser, E.P. Urriolabeitia, One-step microwave synthesis of palladium-carbon nanotube hybrids with improved catalytic performance, Carbon 49 (2011) 652–658, https://doi.org/10.1016/j.carbon.2010.10.012.
[72] D. Albani, M. Shahrokhi, Z. Chen, S. Mitchell, R. Hauert, N. López, J. Pérez-Ramiírez, Selective ensembles in supported palladium sulfide nanoparticles for alkyne semi-hydrogenation, J. Nat. Commun. 9 (2018), 2634, https://doi.org/10.1038/s41467-018-05052-4.
[73] A.J. Murray, J. Zhu, J. Wood, L.E. Macaskie, A novel biorefinery: Biorecovery of precious metals from spent automotive catalyst leachates into new catalysts effective in metal reduction and in the hydrogenation of 2-pentyne, Min. Eng. 113 (2017) 102–108, https://doi.org/10.1016/j.mineng.2017.08.011.
[74] A.J. Murray, J. Zhu, J. Wood, L.E. Macaskie, Biorefining of platinum group metals from model waste solutions into catalytically active bimetallic nanoparticles, Microb. Biotechnol. 11 (2018) 359–368, https://doi.org/10.1111/1751-7915.13030.
[75] S. Shmidt, L.V. Mametova, Main features of catalysis in the styrene phenylation reaction, Kin. Catal. 37 (1996) 406–412.
[76] M.T. Reetz, E. Westermann, Phosphane-free palladium-catalyzed coupling reactions: the decisive role of Pd nanoparticles, Angew. Chem. Int. Ed. 39 (2000) 165–168, https://doi.org/10.1002/(SICI)1521-3773(20000103)39:1<165::AID-ANIE165>3.0.CO;2-B.
[77] B.H. Lipshutz, S. Tasler, W. Chrisman, B. Spliethoff, J. Tesche, Nickel-on-charcoal-catalyzed aromatic aminations and kumada couplings: mechanistic and synthetic aspects, J. Org. Chem. 68 (2003) 1177–1189, https://doi.org/10.1021/jo020297e.
[78] K. Deplanche, M. Merroun, M. Casadesus, T. Tran, I.P. Mikheenko, J.A. Bennett, J. Zhu, J. Wood, I.P. Jones, G.A. Attard, S. Selenska-Pobell, L.E. Macaskie, Microbial synthesis of core/shell gold/palladium nanoparticles for applications in green chemistry, J. Roy. Soc. Interface 9 (2012) 1705–1712, https://doi.org/10.1098/rsif.2012.0003.
[79] P.J. Ellis, I.J.S. Fairlamb, S.F.J. Hackett, K. Wilson, A.F. Lee, Evidence for the surface catalysed Suzuki-Miyaura reaction over palladium nanoparticles: an operando XAS study, Angew. Chem. Int. Ed. 49 (2010) 1820–1824, https://doi.org/10.1002/anie.200906675.
[80] C.G. Baumann, S. De Ornellas, J.P. Reeds, T.E. Starr, T.J. Williams, I.J.S. Fairlamb, , Formation and propagation of well defined palladium nanoparticles (PdNPs) during C-H bond functionalization of heteroarenes: are nanoparticles a moribund form of Pd or an active catalyst species? Tetrahedron 70 (2015) 6174–6187, https://doi.org/10.1016/j.tet.2014.06.002.
[81] L.E. Macaskie, K.M. Bonthrone, P. Yong, D. Goddard, Enzymically mediated bioprecipitation of uranium by a Citrobacter sp.: a concerted role for exocellular lipopolysaccharide and associated phosphatase in biomineral formation, Microbiol 146 (2000) 1855–1867, https://doi.org/10.1099/00221287-146-8-1855.
[82] L.E. Macaskie, J. Collins, I.P. Mikheenko, J. Gomez-Bolivar, M.L. Merroun, J. A. Bennett, Enhanced hydrogenation catalyst synthesized by *Desulfovibrio desulfuricans* exposed to a radio frequency magnetic field, Microb. Biotechnol. 14 (2021) 2041–2058, https://doi.org/10.1111/1751-7915.13878.
[83] Á. Molnár, Efficient, selective, and recyclable palladium catalysts in carbon−carbon coupling reactions, Chem. Rev. 111 (2011) 2251–2320, https://doi.org/10.1021/cr100355b.
[84] S. Jagtap, Heck reaction - state of the art, Catalysts 7 (2017) 267–320, https://doi.org/10.3390/catal7090267.
[85] H.E. Bonfield, D. Valette, D.M. Lindsay, M. Reid, Stereoselective remote functionalization via palladium-catalyzed redox-relay Heck methodologies, Chem. Eur. J. 27 (2021) 158–174, https://doi.org/10.1002/chem.202002849.
[86] M.M.TNamboodiri, K. Pakshirajan Ch 10 inIntegrating Biorefineries for Waste Valorization, in: T. Bhaskar, A. Pandey,E:R. Rene, D:W. Tsang (Eds.), Elsevier, 2020, 241–266.
[87] X. Moreau, J.M. Campagne, G. Meyer, A. Jutand, Palladium-catalyzed C-S bond formation: rate and mechanism of the coupling of aryl or vinyl halides with a thiol derived from a cysteine, Eur. J. Org. Chem. 2005 (2005) 3749–3760, https://doi.org/10.1002/ejoc.200500227.
[88] P.S. Haradem, J.L. Cronin, R.A. Krause, L. Katz, Chemical and structural characterization of a palladium polysulfide, $(NH_4)_2PdS_{11}\cdot 2H_2O$ Inorg, Chim. Acta (25) (1997) 173–179, https://doi.org/10.1016/S0020-1693(00)95708-6.
[89] R.A. Krause, A.W. Kozlowski, J.L. Cronin, in: J.P. Fackler Jr (Ed.), Polysulfide Chelates. in Inorganic Synthesis, John Wiley & Sons, 1982, pp. 12–18.
[90] R. Steudal, T. Chivers, The role of polysulfide dianions and radical anions in the chemical, physical and biological sciences, including sulfur-based batteries, Chem. Soc. Rev. 48 (2019) 3279–3319, https://doi.org/10.1039/c8cs00826d.
[91] G.S. Pokrovski, M.A. Kokh, D. Guillaume, A.Y. Borisova, P. Gisquet, J.-L. Hazemann, E. Lahera, W. Del Net, O. Proux, D. Testemale, V. Haigis, R. Jonchiere, A.P. Seitsonen, G. Ferlat, R. Vuilleumier, A.M. Saitta, M.-C. Boiron, J. Dubessy, Sulfur radical species form gold deposits on Earth, Proc. Nat. Acad. Sci. USA 112 (2015) 13484–13489, https://doi.org/10.1073/pnas.1506378112.
[92] F. Reith, G. Nolze, R. Saliwan-Neumann, B. Etschmann, M.R. Kilburn, J. Brugger, Unravelling the formation histories of placer gold and platinum-group mineral particles from Corrego Bom Successo, Brazil: a window into noble metal cycling, Gondwana Res. 76 (2019) 246–259, https://doi.org/10.1016/j.gr.2019.07.003.
[93] I.J. Pickering, G.N. George, E.Y. Yu, D.C. Brune, C. Tuschak, J. Overmann, Analysis of sulfur biochemistry of sulfur bacteria using X-ray absorption spectroscopy, Biochemistry 40 (2001) 8138–8145, https://doi.org/10.1021/bi0105532.
[94] Resource Recovery from Wastes: Towards a Circular Economy, L.E. Macaskie, D.J. Sapsford, W.M.Mayes (Eds.), Green Chemistry Series No 63, Royal Society of Chemistry London, 2020. ISBN: 978-1-78801-381-9.
[95] Anon. Resources and Waste Strategy for England Department for Environment Food and Rural Affairs, HM Government UK 2018 Ref PB 14552 ⟨https://www.gov.uk/government/publications/resources-and-waste-strategy for England⟩. (Accessed 18 July 2020).